Western Kentucky University

TopSCHOLAR®

Spring 2021

Synthesis and Catalytic Oxidation of Organic Substrates by Light-Harvesting Metalloporphyrins

Christian Alcantar
Western Kentucky University, christian.alcantar238@topper.wku.edu

Follow this and additional works at: https://digitalcommons.wku.edu/theses

Part of the Inorganic Chemistry Commons, and the Organic Chemistry Commons

SYNTHESIS AND CATALYTIC OXIDATION OF ORGANIC SUBSTRATES BY
LIGHT-HARVESTING METALLOPORPHYRINS

A Thesis
Presented to
The Faculty in the Department of Chemistry
Western Kentucky University
Bowling Green, Kentucky

In Partial Fulfillment
Of the Requirements for the Degree
Master of Science
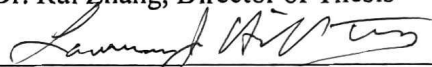
By
Christian Alcantar

May 2021

SYNTHESIS AND CATALYTIC OXIDATION OF ORGANIC SUBSTRATES BY LIGHT-HARVESTING METALLOPORPHYRINS

Date Recommended 04-15-2021

_____
Dr. Rui Zhang, Director of Thesis

_____
Dr. Lawrence Hill

_____
Dr. Kevin Williams

i   v   i

I dedicate this thesis to my wonderful wife and my beautiful little girls.

ACKNOWLEDGMENTS

efforts in keeping safe all the budding chemists, future health care workers, and all the other future professionals who populate the chemistry lab courses. Most of all, I appreciate the enjoyable conversations, helpful advice, calming encouragement, and interesting stories that she has taken the time to share. I will truly miss these two integral members of the chemistry department and all-around wonderful people.

My time here at WKU has brought me many friends for whom I am greatly happy to have found. I am especially thankful to have met Fox Bratcher and Seth Klaine. As my fellow researchers and longest-running and closet friendships in the department, I am deeply grateful for their support in keeping me afloat during my time in graduate school as well as their aid in the kinetics and catalytic studies of this work. I have greatly benefitted from Fox's research ingenuity and from observing the creativity of someone who has found in chemistry more than a job, but a passion and hobby. I have also greatly benefitted from Seth's experience and advice as well as him always being there to annoy with questions and possessing a depth of knowledge in chemistry surpassing that of what would be expected for someone his age. I would also like to thank my other current colleagues for their support and friendship: Mardan Khashimov, Iyanu Ojo, Tristan Skipworth, and Jason Zhang. I am also grateful toward both Jonathan Malone and Davis Ranburger for their training in my undergraduate. As well, I am glad to have worked alongside many other previous coworkers and friends: Ben Willis, Wentao Ning, Angeline Dames, Ben Kash, and Stuart Kernohan.

I would also like to acknowledge the Distinguished Minority Fellows program for providing me with a much needed scholarship, as well as the National Science Foundation

Finally, I would like to thank those in my church and campus ministry for providing me with support in the most important areas of my life and keeping me focused on the end goal. I would not be who I am, nor would I have the potential to be who I could be, without the time I have spent with them. Most importantly, I thank my family for seeing me through this time and providing me with amazing and generous support and care for which I feel is far beyond what anyone could deserve. To my mother Joan and father Quetza, I am grateful to have such wonderful parents. To my little girls, I am so excited to be watching you grow up into wonderful and godly young women; using this degree to help provide for you was one of my main motivations. To my most loving Mary, to whom I am ready to dedicate the rest of my life to and who never stopped encouraging me with love, prayer, and care, I love you with all my heart. Better together.

TABLE OF CONTENTS

LIST OF TABLES

LIST OF FIGURES

LIST OF SCHEMES

SYNTHESIS AND CATALYTIC OXIDATION OF ORGANIC SUBSTRATES BY LIGHT-HARVESTING METALLOPORPHYRINS

Christian Alcantar   May 2021   54 Pages

Directed by: Dr. Rui Zhang, Dr. Kevin Williams, and Dr. Lawrence Hill

Department of Chemistry   Western Kentucky University

In this work, ruthenium, iron, and manganese light-harvesting metalloporphyrins have been successfully synthesized to serve as biomimetic models of the active site of Cytochrome P450 for the development of a green and efficient oxidation catalyst. The covalent introduction of light-harvesting boron-dipyrrin (BODIPY) fluorophores on the porphyrin macrocycle allows for the absorption of a broader range of visible light in addition to that captured by the porphyrin aromatic system alone. It is expected that this core-antenna system will increase the absorbed light energy and transfer it to the reaction center, and thereby increase the efficiency of the catalyst. Fluorescence spectrometry was used to identify the presence of energy transfer from the BODIPY units to the porphyrin core, in which the fluorescence spectrum of the BODIPY overlaps with the absorbance spectra of the porphyrin chromophore at the Q band region.

The manganese(IV)-oxo light-harvesting porphyrin was also formed by both photochemical and chemical oxidation of the manganese(III) precursors. A kinetic plot of the observed rate constants for the reaction of manganese(IV)-oxo light-harvesting porphyrin with varying concentrations of thioanisole shows a linear relationship where the slope gives the second-order rate constant k_{ox} ($M^{-1}s^{-1}$) = 0.4158, which was contrary to what

was expected given the greater range of light energy able to be utilized. Ruthenium, iron, and manganese light-harvesting porphyrins served as oxidation catalysts that underwent preliminary oxidation trials with both sulfide and alkene substrates. In the presence of visible light, the ruthenium BODIPY porphyrin displayed an enhanced catalytic activity for both the sulfoxidation and epoxidation with $PhI(OAc)_2$ and 2,6-dichloropyridine *N*-oxide as oxygen sources, respectively. The epoxidation and sulfoxidation reactions catalyzed by both iron and manganese, however, fell below expectations. Possible explanations for the lack of reactivity include stable µ-oxo dimer formation or photodegradation of the catalysts.

1.1   Overview of Cytochrome P450 Enzymes

Cytochrome P450 enzymes (CYP450) have been a subject of rigorous study for decades. Research involving CYP450 spans back to a time before it was officially discovered even to 1948 with Mueller and Miller researching the metabolism of carcinogens.[1] It first gained attention as a hepatic enzyme able to catalyze the demethylation of the medication ephedrine in the presence of molecular oxygen.[2,3] Later works with this same entity identified the ability to bind to carbon monoxide and displayed a strong spectral peak at 450 nm.[4,5] The suggested classification of this enzyme as a new cytochrome heme enzyme came in 1962 from preliminary work by Omura and Sato, in which it was given the name of P450 for the absorbance maxima at 450 nm and further confirmed again in 1964 by the same authors.[6,7] The same works noted the ability of P450 to rapidly reoxidize upon exposure to molecular oxygen.

Over half a century of study and technological advancement has advanced to a more thorough and accurate knowledge of CYP450s. Today, we understand CYP450 as an enzyme superfamily of heme-binding monooxygenases consisting of tens of thousands of members found throughout the majority of living organisms such as mammals, plants, and some bacteria (Figure 1-1). These enzymes are responsible for a variety of critical oxidative processes necessary for life.[8,9] To our current understanding, CYP450s perform two main functional roles. The first is the metabolism of xenobiotics, in which exogenous molecules are oxidized to increase aqueous solubility in preparation for excretion for the protection

of the organism. This includes the processing of drugs, poisons, herbicides, insecticides, etc. As well, enzymes of this superfamily participate in the biosynthesis of signaling molecules in the body.[10]
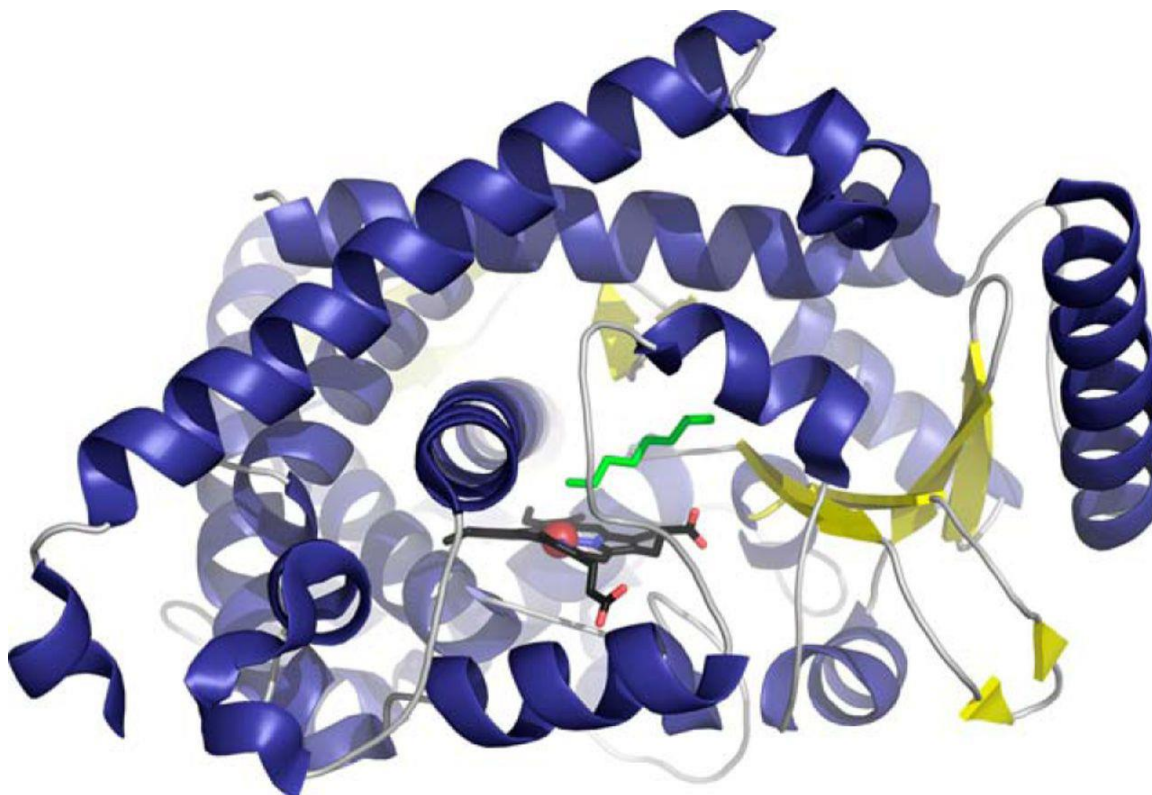
Figure 1-1. Simulated structure of cytochrome P-450s.[11]

The roles of these CYP450 enzymes in xenobiotic metabolism and biosynthesis necessitate the ability to perform various types of organic substrate oxidations. Such oxidations include oxidation of sulfides into sulfoxides, epoxidation of olefins, oxidation of aromatics, and even hydroxylations of normally inert saturated hydrocarbon bonds, as well as many more (Figure 1-2).[12] In order to perform these oxidations, CYP450 is able to make use of normally inert molecular oxygen, inserting one oxygen atom onto the substrate while reducing the other to a water molecule with electrons donated from NAD(P)H. The ability for these enzymes to utilize molecular oxygen involves the modification of the

electronic structure of dioxygen out of the triplet state through the binding of the molecule

to the active site of the enzyme.[13]
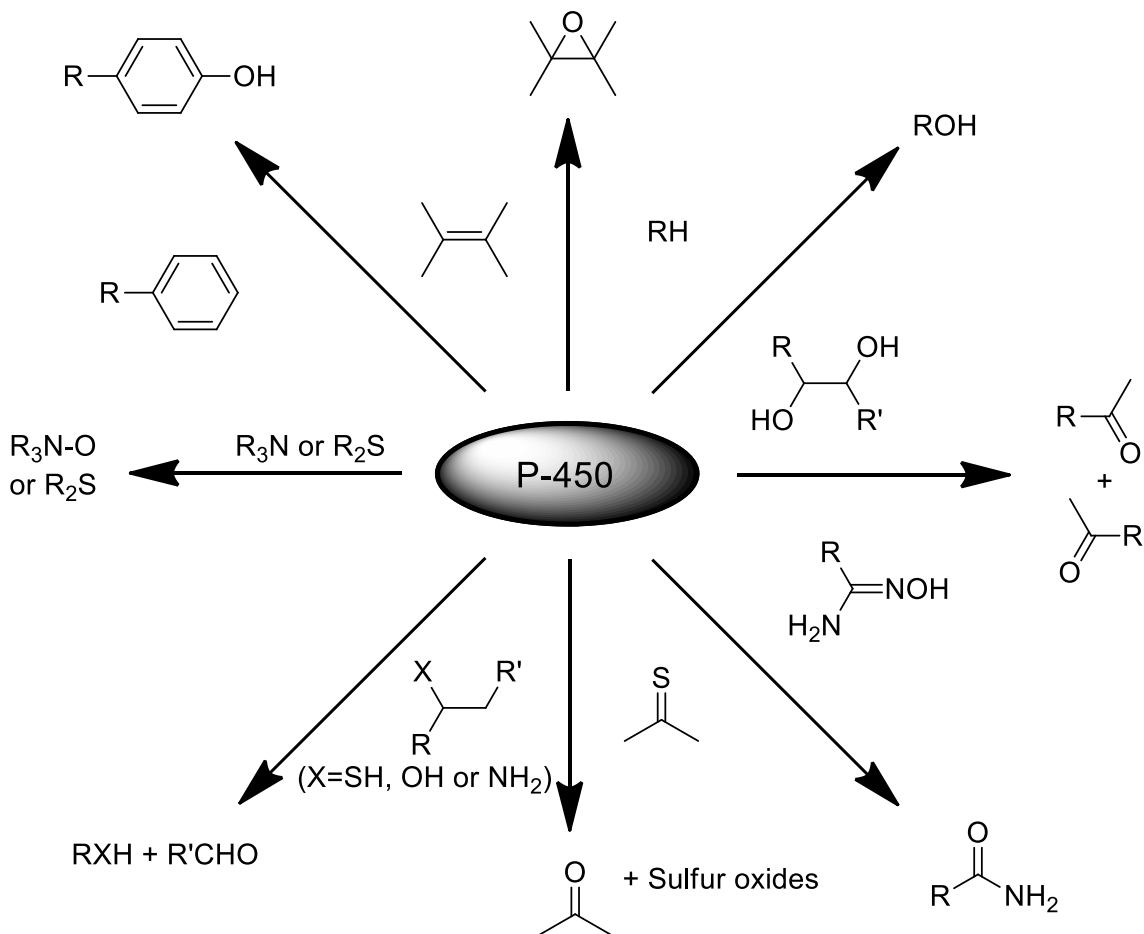
Figure 1-2. Types of organic substrate oxidations catalyzed by cytochrome P-450. Recreated from Ji and Zhou.[13]

The oxidative transformations performed by CYP450s utilize an iron(III) protoporphyrin-

IX as a heme prosthetic group for the active site in which the molecular oxygen is bound

as shown in Figure 1-3. This metal atom encompassed in a tetrapyrrolic frame is a common

structure for various biological processes performed throughout nature. Examples include

the light-capturing chlorin structure found in chlorophyll, the most broadly occurring

natural macrocycle; as well as corrin, the nineteen-carbon porphyrin analog existing as the

3

main structure in vitamin B12.[14,15] The porphyrin macrocycle acts as a ligand encompassing an iron(III) atom with nitrogen groups of the pyrrole subunits bonded to the metal center. In the axial position of the heme structure is a cysteine thiolate ligand contributing to the oxidative potential of the iron group and acting as a bridge to the protein structure.[16,17]
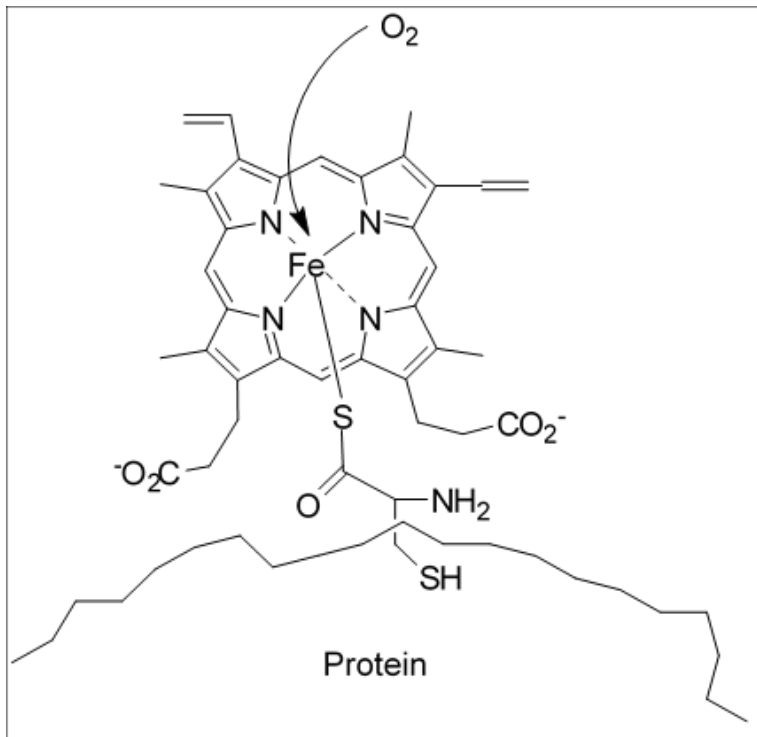
Figure 1-3. Approximation of the general design of the heme-structure demonstrating its location on the cytochrome protein and the thiolate bridge connection. Reproduced from Ji and Zhou.[13]

The catalytic cycle of CYP450 and its various oxo-intermediates has been the subject of much study.[16,18,19] This research has aided in the elucidation of the oxidative pathway as shown in Scheme 1-1. The cycle begins with the enzyme in a low-spin state as iron(III) with a water molecule axial ligand. A substrate displaces the water molecule transitioning the iron to a higher spin-state followed by a single-electron reduction from NAD(P)H to the iron center transitioning it to iron(II) followed by the binding of molecular oxygen to

form an iron(III) superoxide intermediate. Another electron reduction and protonation of the distal oxygen leads to an anionic peroxy-intermediate known as Compound 0. A second protonation of the distal oxygen and subsequent heterolytic scission of the peroxide bond yields water and the notable high-valent radical cationic iron(IV) species termed Compound I. Hydrogen atom abstraction from the substrate generates a substrate radical and a less reactive neutral iron(IV) species termed Compound II. Finally, hydroxylation of the substrate and water molecule ligation regenerates the resting state of the enzyme.[16,20] A few alternative pathways exist at various points in the catalytic cycle that may return the enzyme to the resting state without completing the traditional cycle.[21]
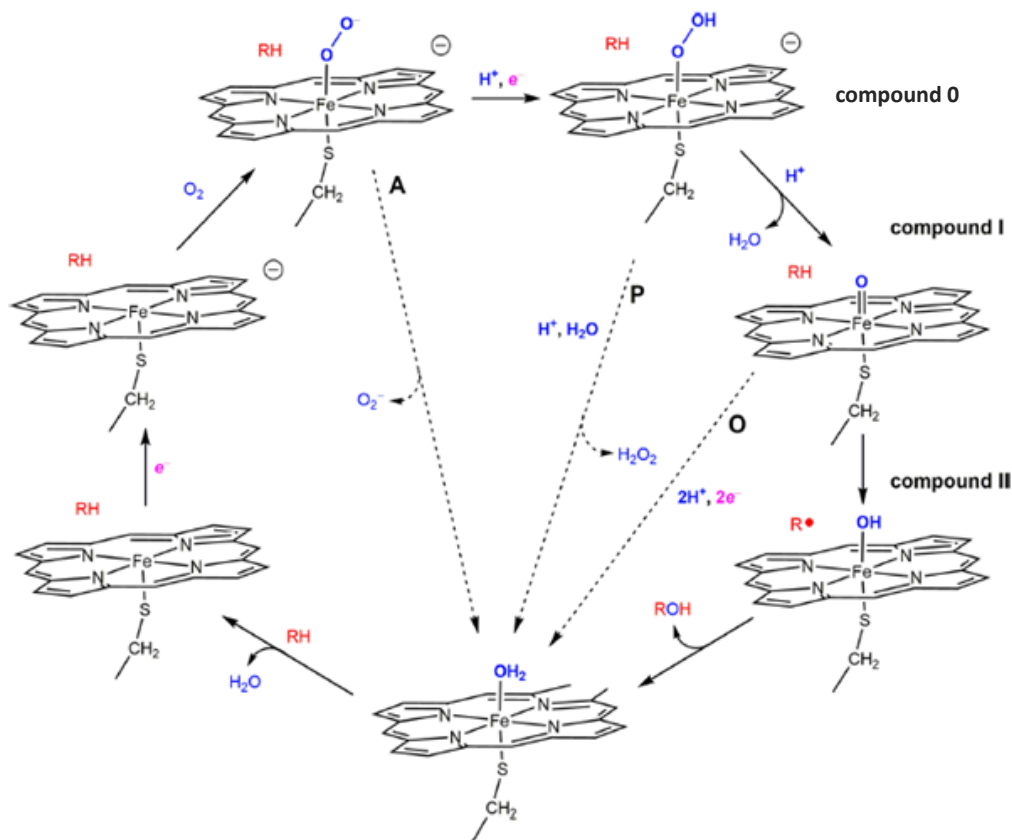
Scheme 1-1 Cytochrome P450 catalytic cycle. Three non-productive short circuits (dashed lines): autoxidation (A), peroxide shunt (P), and oxidase (O) pathways. Modified from Gray and Winkler.[16]

1.2   Biomimetic Models of Cytochrome P450s

There is considerable interest in the understanding of complex reaction pathways and mechanisms in which CYP450 operates. Aside from being a ubiquitous and integral entity for the majority of life on Earth, these enzymes are able to perform efficient oxidation on such a wide variety of organic compounds with high regio-, chemo-, and stereoselectivity. Furthermore, the ability to activate molecular oxygen for use in oxidative transformations is a significant point of interest that caused many to seek broader insights into the biochemical processes of these enzymes.[13]
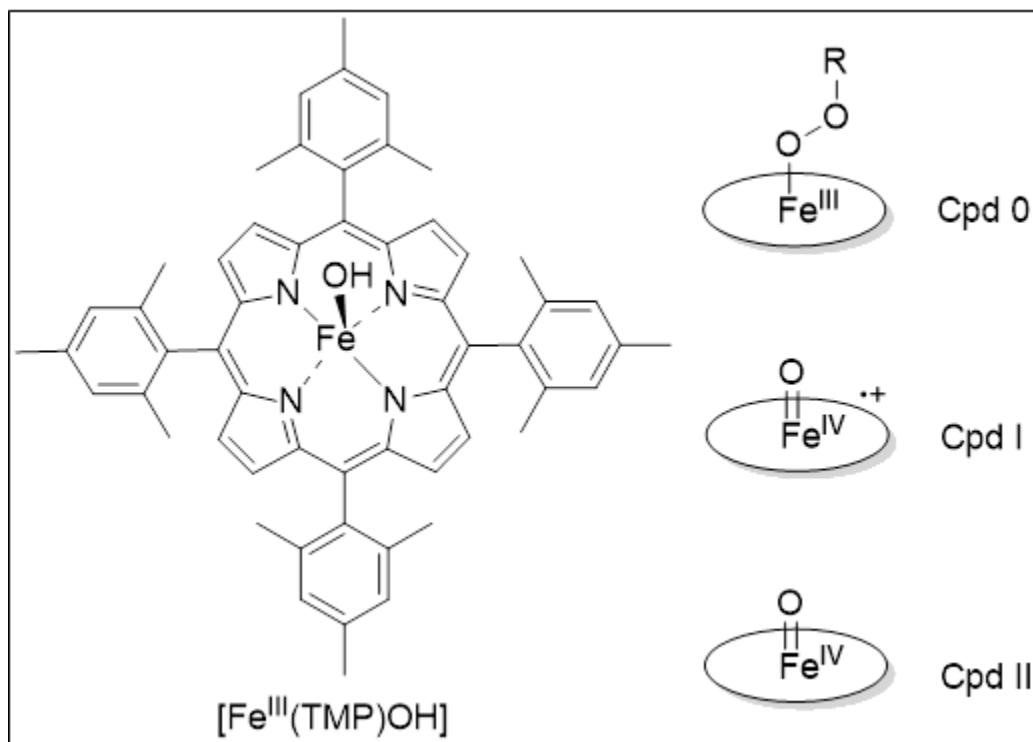
Scheme   1-2   Iron(III)   5,10,15,20-tetrakis(2,4,6-trimethylphenyl)porphyrin hydroxide where TMP = tetrametsityl porphyrin (left). Compounds 0 (top right), I (middle right), and II (bottom right). The R group represents the rest of an mCPBA on Compound 0. Reproduced from Fertinger *et al*.

In the past, investigations into CYP450 and its oxidative capabilities involved experiments using actual CYP450 enzymes requiring the isolation of the hepatic enzymes from biological sources.[22] However, given the difficulty of extraction, isolation, and purification processes for biological complexes, there exists a need for a simpler synthetic equivalent. It is well-known that the active site of the CYP450 enzyme on which the oxygen atom transfer (OAT) takes place consists of an iron-protoporphyrin IX complex. This complex forms several prevalent high-valent iron-oxo intermediates as the enzyme progresses through the catalytic cycle, namely those intermediates termed Compounds 0, I, and II. Each of these compounds can act as an active oxidation species depending on the conditions and substrate, as noted by the varying branches in the catalytic cycle as shown in Scheme 1-1. Of the three main intermediates, the high-valent iron(IV)-oxo porphyrin radical cationic species, i.e. Compound I, is considered to be the most potent oxidant and is postulated to serve as the premier oxidant for the catalytic cycle.[23–25] Biomimetic models of these iron-oxo porphyrin species within the active site have been synthesized and studied for decades to allow for an enhanced understanding of the oxidation mechanisms of this ubiquitous enzyme superfamily and the catalytic properties of the reactive intermediates (Scheme 1-2).[23,26]

Metalloporphyrins have undergone a rich evolution over the years since their initial utilization as synthetic analogs to the protoporphyrin IX core of the CYP450 active site.[27] It was found that the simplest forms of these complexes, containing only a porphyrin macrocycle bound as a ligand to an iron atom, were not efficient catalysts for oxidation; the porphyrin ring behaves like a more reactive substrate leading to self-hydroxylation of the species. However, it was found that the addition of substituents at the *meso*-positions

of the macrocycle defends against this catalyst bleaching as well as allows for tuning of the electronic environment of the catalyst with substituents of varying electronic natures.[28]

Research performed by Rothemund in 1936 is often considered to have laid the foundation for the synthesis of *meso*-substituted porphyrin free-ligand.[29,30] Rothemund's method of synthesis utilized reactions of pyrrole with various aldehydes. The porphyrin structures that were synthesized have come to be known as first-generation porphyrin structures as described by Dolphin and Traylor in which only simple substituents such as substituted phenyl groups exist on the *meso*-positions of the macrocycle.[31] The Rothemund method of synthesis required reaction times of up to 48 hours and resulted in low yields and a narrow scope on the variations of the porphyrin substituents. Decades later, Adler *et al.* published an improved synthesis method for a wide variety of non-sterically hindered *meso*-substituted porphyrins. Adler's method of free ligand synthesis resulted in higher yields and reduced the reaction time from days to minutes.[32,33] Another major milestone was set by the work of Lindsey *et al* who established efficient methods for obtaining porphyrin free ligand bearing sterically-hindered *ortho*-substituted phenyl groups.[34,35] The methods published by Adler and Lindsey have continued to be utilized for the synthesis of the CYP450 active site analogs.[36,37]

This new catalyst design using substituents on the phenyl groups attached to the *meso*-position of the macrocycle is considered as the second generation of porphyrin catalysts. With the functionalization of the phenyl groups, the electronic environment of the catalyst is altered changing its catalytic properties after undergoing the insertion of a metal. This allows for the increase or decrease in the electrophilicity of the metal center as well as altering the catalyst stability and redox potential.[31,38,39] Further halogenation of the

porphyrin macrocycle on the β-position constitutes the third generation metalloporphyrins. All three generations of metalloporphyrin catalysts are shown in Figure 1-4.
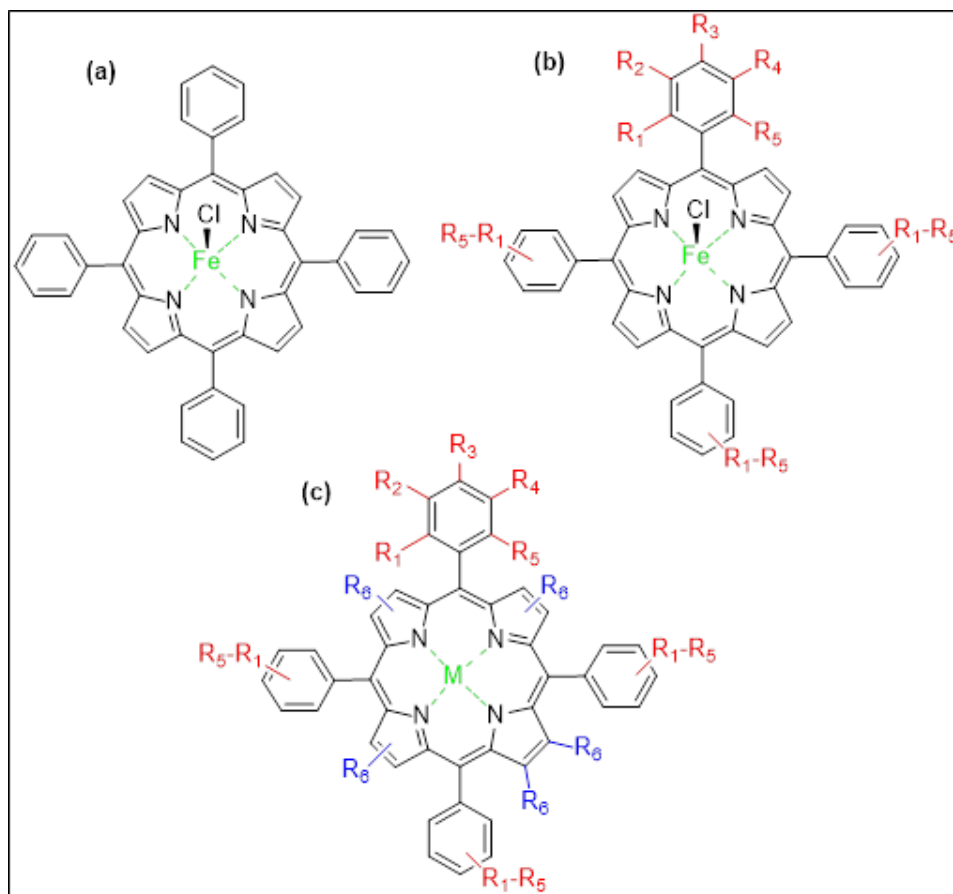
Figure 1-4. Metalloporphyrin generations: first generation (a), second generation (b), and third generation (c). Retrieved from Barona-Castaño.[27]

The high-valent iron(IV) radical cationic species termed Compound I is noted to be the most reactive of the oxo-intermediates within the CYP450 catalytic cycle and is postulated to act as the primary active oxidant within the cycle.[23,24] Biomimetic analogs of these compounds have served as useful models for CYP450 research and selective oxidation catalyst design. The first reported synthesis and characterization of a synthetic Compound I model were published by Groves *et al*. The iron porphyrin was used to catalyze the hydroxylation and epoxidation of hydrocarbons using iodosylbenzene as a

sacrificial oxidant. This work paved the way for a new direction in biomimetic oxidation catalysis becoming a point of reference for many academic researchers for decades afterward who will expand on the work and varying the catalyst design in substituents, macrocyclic structure, axial ligand, and exchanging the iron center with other metals, among many other aspects.[36,40,41]

Much interest has been garnered from manganese porphyrin catalysts. Manganese porphyrin complexes are more active compared to their iron counterparts and so tend to be used in the creation of CYP450 model systems. Early examples of this can be seen in work published by Weschler *et al* in which a *meso*-tetraphenylporphyrin(pyridine)manganese(II) complex is generated and isolated in order to study the reversible adduct formation of the manganese porphyrin and dioxygen. Further, Groves *et al* in 1980 indicated that Mn(V)-oxo porphyrin complexes could be generated for catalytic epoxidation and hydroxylation, showing promise.[41,42] It has been shown that Mn(V)-oxo intermediates are more reactive than even the Fe(IV)-oxo cationic radical species.[43,44]

In a similar vein, ruthenium porphyrin complexes have been of great interest. Computational studies suggest that a ruthenium(IV)-oxo species could be relatively stable. As well, Ru(V)-oxo species have demonstrated potential for aerobic photochemical oxidation formed via a disproportionation mechanism. It demonstrated high reactivity in comparison with Compound I analogs. Ruthenium porphyrin shows great potential in the search for a greener, more robust oxidative catalyst.[45–47]

1.3   Importance of Oxidation Reactions

Oxidative transformations are integral and commonplace processes in a multitude of fields such as pharmaceutical production, organic synthesis, polymer chemistry, and petrol

chemistry. [48–50] The C-H oxidation is of particular interest to many within industry given the resources available, such as petroleum-based constituents such as oil and natural gas, which can serve as large chemical feedstocks. Oxidation is a useful method for the functionalization of hydrocarbons, such as saturated alkanes, olefins, and aromatic compounds into useful oxidized products such as epoxides, alcohols, and carbonyl compounds. It also opens the door to further transformations of inert petroleum constituents into other useful chemical products. Millions of tons of these products are produced globally and find uses in multiple chemical industries. [51,52]

As well, there has been growing attention in the process of sulfide oxidation and applications of sulfoxides. The selective oxidation of sulfur compounds is a valuable transformation within industry as these sulfoxide compounds are the intermediates for many biologically active molecules and pharmaceuticals such as anti-bacterials, anti-ulcers, and psychotonics, among others. [53–56] Sulfoxide-containing complexes can also be utilized for chemical synthesis such as with functional group transformations, oxidations, or use as a solvent such as dimethylsulfoxide. [57,58] The oxidation of sulfides is also of interest for the removal of sulfide contaminants in fuels. Combustion of unreformed fuel can lead to poisoning of the platinum converter in vehicles and the release of toxic sulfur dioxide. Oxidation of the sulfide contaminants allows for easier removal. [59–61]

Catalysis has been in use for many important industries for hundreds of years and has undergone significant evolution in that time. [62] A significant portion of global gross product relies on catalysis, such as those involved with chemicals and fuels. [63] Catalytic oxidation is an important subcategory within industrial catalysis. The pharmaceutical industry currently employs many large-scale catalytic oxidation processes for drug production. [64]

11

However, many current methods of oxidation leave much to be desirable. For the production of sulfoxides, often the most common reagents used can lead to over-oxidation to sulfone. For sulfoxide formation, the reaction conditions must necessarily be tailored to reduce the production of this over-oxidized product.[65] There is a need for greener, more robust catalysts that can efficiently and selectively oxidize organic substrates.

CHAPTER 2

EXPERIMENTAL SECTION

2.1   Materials

All commercial reagents were of the best available purity and utilized as received unless otherwise noted. All solvents including dichloromethane, hexane, ethyl acetate, methanol, acetone, acetonitrile, ethanol, *N,N*-dimethylformamide, propionic acid, toluene, dichloroethane, 1,2,4-trichlorobenzene, and chloroform were purchased from Sigma-Aldrich Chemical Company or Fisher Scientific and utilized as received. Pyrrole and 2-methylpyrrole were purchased from Sigma-Aldrich Chemical Company and freshly distilled before synthesis. Substrates used for catalytic oxidations were used as purchased from Sigma-Aldrich Chemical Company including thioanisole, 4-fluorothioanisole, 4-chlorothioanisole, 4-methylthioanisole, 4-methoxythioanisole, diphenyl sulfide, styrene, 4-fluorostyrene, 4-chlorostyrene, 4-methtylstyrene, cis-cyclooctene, and cis-stilbene. Trifluoroacetic acid (TFA), p-cyanobenzaldehyde, sodium hydroxide, sodium sulfate, diisobutylaluminum hydride (DIBAL-H), ammonium chloride, 2,3-dichloro-5,6-dicyano-p-benzoquinone (DDQ), triethylamine, boron trifluoride diethyl etherate (BF$_3$·OEt$_2$), iodobenzene diacetate [PhI(OAc)$_2$], triruthenium dodecacarbonyl [Ru$_3$(CO)$_{12}$], iron(II) chloride (FeCl$_2$), manganese(II) acetate tetrahydrate [Mn(OAc)$_2$·4H$_2$O], and chloroform-*d* were all used as purchased from Sigma-Aldrich Chemical Company.

2.2   Instrumentation

Gas chromatography-mass spectrometry (GC-MS) analysis was performed using an Agilent GC6890-MS5973 equipped with a flame ionization detector (FID) using a J&W DB-5 capillary column and an automatic sample injector. UV-vis spectra were recorded

using an Agilent 8453 diode array spectrophotometer. Fluorescence spectra were obtained using a PerkinElmer LS-55 spectrometer. ^{1}H-NMR spectra were obtained using a JEOL ECA-500 MHz spectrometer at 238K with tetramethylsilane (TMS) as the internal standard in deuterated chloroform (CDCl$_3$) as the solvent. The chemical shifts (ppm) were reported relative to the TMS standard peak.
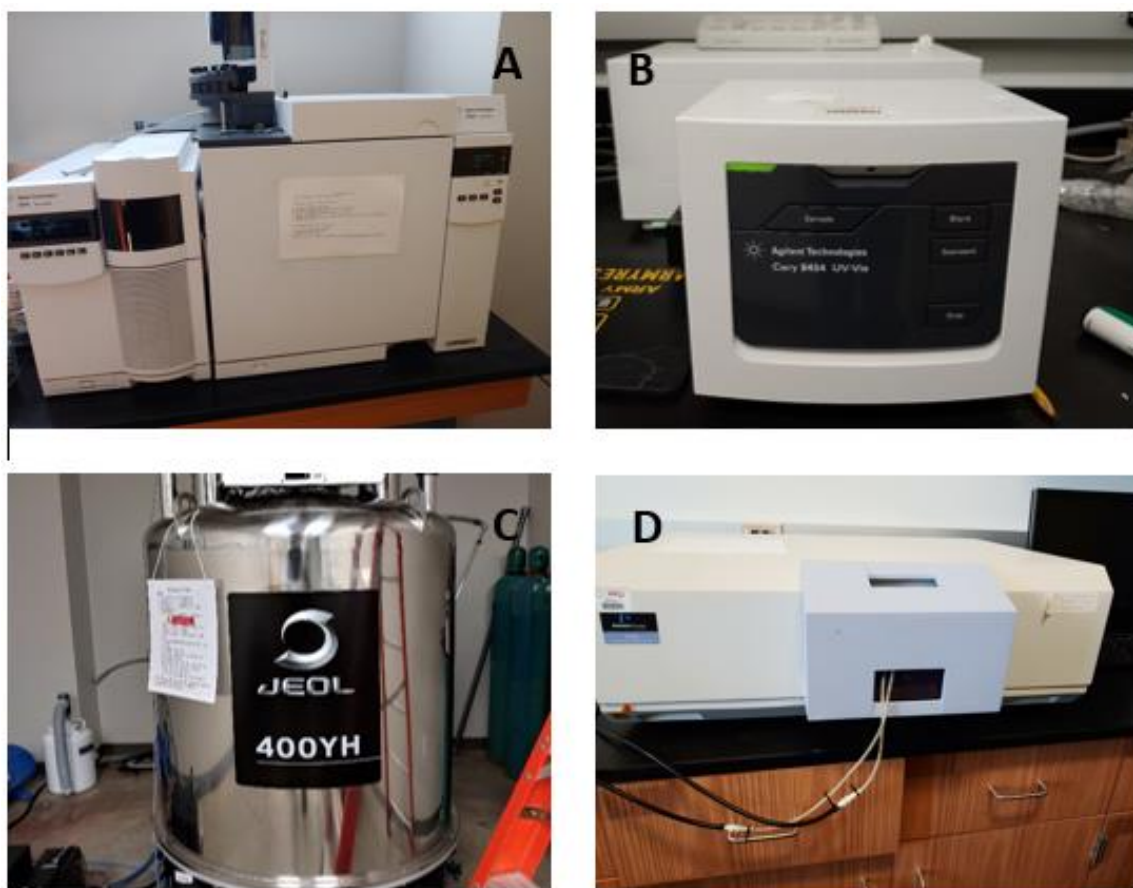
Figure 2-1. (A) Agilent GC6890-MS5973. (B) Agilent 8453 diode array spectrophotometer. (C) JEOL ECA-500 MHz spectrometer. (D) PerkinElmer LS-55 spectrometer.

2.3   Methods

2.3.1   Reagent Purification

Commercially available pyrrole and 2-methylpyrrole were separately distilled for purification. Pyrrole (*ca*. 10 mL) was added to a 25 mL round-bottom flask fitted with a water-jacketed distillation head and a magnetic stir bar. The solution was heated between 100 ºC to 120 ºC and the colorless distillate was collected. The purified pyrrole was used for porphyrin synthesis and 2-methylpyrrole for the light-harvesting aldehyde synthesis.

2.3.2   General Procedure for Catalytic Oxidations

Photocatalytic reactions were performed using the synthesized metalloporphyrins complexes to determine catalytic efficiency for the oxidation of various organic substrates including various *p*-substituted thioanisoles and *p*-substituted styrenes as well as a few other related alkenes. The reactions were performed using a Rayonet photoreactor (RPR-100) capable of a wavelength range of 400-500 nm (λ_{max} at 419 nm) using 300 W mercury lamps (RPR-4190 × 12). Sulfide oxidation procedure generally involved the addition of 0.2 mol% catalyst being loaded into a solution of methanol or chloroform (2 mL) containing $PhI(OAc)_2$ (0.75 mmol) and the sulfide substrate (0.5 mmol) in a ratio of 3:2 oxygen source to substrate in the presence of a small amount of water (4.5 µL). The solution was then irradiated at 25 ± 2 ºC using the Rayonet photoreactor. Alkene epoxidation followed a similar procedure involving 0.1 mole% of catalyst loaded into a solution of dichloromethane (2 mL) with 2,6-dichloropyridine *N*-oxide (0.55 mmol) and alkene substrate (0.5 mmol). Aliquots of the reaction solutions were taken at constant time intervals and analyzed on GC-MS to determine product yields and selectivity.

2.4 Light-harvesting Aldehyde Synthesis
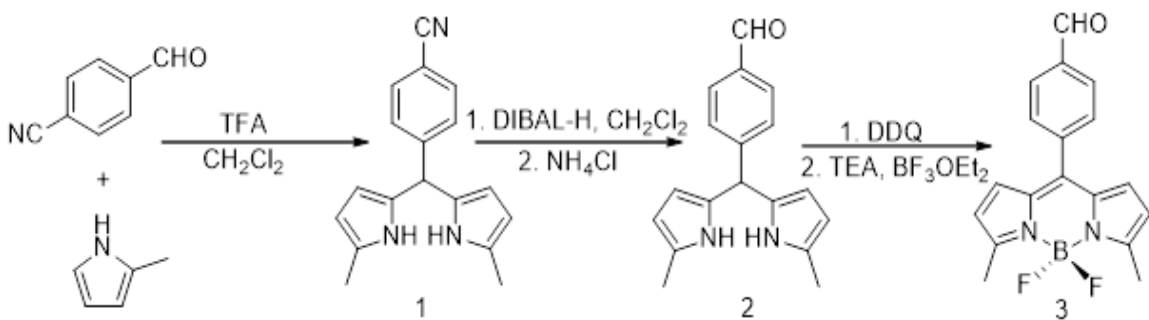
Scheme 2-1. The three-step synthesis of the light-harvesting aldehyde (**3**)

2.4.1 Synthesis of 1,9-Dimethyl-5-(4-cyanophenyl)dipyrromethane (1)

The synthesis of the light-harvesting aldehyde (**3**) is derived from methods reported by Dolphin in 2009 with minor modifications.[66] Freshly distilled 2-methylpyrrole (3.125g, 37.0 mmol) and 4-formylbenzonitrile (2.53 g, 18.3 mmol) were dissolved in dichloromethane (87 mL) and degassed with argon for 10 minutes and treated with trifluoroacetic acid (211 μL, 2.75 mmol). The solution was stirred at room temperature for 3 hours and monitored with TLC. The reaction was then quenched with 0.2 M aqueous NaOH (87 mL) and extracted with ethyl acetate. Na_2SO_4 was used to dry the solution and evaporated with rotary evaporation under vacuum. A yellow solid (2.7 g, 54%) was obtained after column chromatography (silica, CH_2Cl_2). ^{1}H-NMR analysis was used to verify the structure and purity (Figure 2-2A).

Yield = 2.7 g (54%)

R_f (silica, CH_2Cl_2): 0.5

^{1}H-NMR (500 MHz, CDCl$_3$): δ, ppm: 7.66 (s, 2H, 2NH); 7.59 (d, 2H, Ar-H); 7.32 (d, 2H, Ar-H); 5.80 (t, 2H, β-pyrrole) 5.68 (t, 2H, β-pyrrole); 5.40 (s, 1H, H-meso); 2.21 (s, 6H, CH$_3$).

16

2.4.2 Synthesis of 1,9-dimethyl-5-(4-formylphenyl)dipyrromethane (2)

In a 500 mL RBF was added (2.7 g, 9.4 mmols), dichloromethane (91 mL), and a large stir bar. The solution was degassed with argon for 10 min. DIBAL-H (1 M in hexanes, 18.9 mL, 18.9 mmol) was added in a dropwise manner into solution and stirred for 4 h at room temperature followed by quenching using saturated aqueous NH_4Cl (122 mL) and stirred for another 2 h. An aqueous solution of NaOH (10%, 122 mL) was added to the solution. Using vacuum filtration, the red solid was removed from the solution. The aqueous phase was extracted using ethyl acetate three times. The combined organic layers were dried with Na_2SO_4 and evaporated on a rotary evaporator. The dried product was purified using column chromatography (silica, CH_2Cl_2). The collected product (1.28 g, 49%) was verified with ^{1}H-NMR analysis (Figure 2-2B), matching literature reported data.

Yield = 1.28 g (49%)

R_f (silica, CH_2Cl_2): 0.36

^{1}H-NMR (500 MHz, CDCl3): δ, ppm: 9.97 (s, 1H, CHO); 7.82 (d, 2H, Ar-H); 7.67 (s, 2H, 2NH); 7.39 (d, 2H, Ar-H); 5.80 (t, 2H, β-pyrrole); 5.72 (t, 2H, β-pyrrole); 5.43 (s, 1H, H-*meso*); 2.21 (s, 6H, CH$_3$)
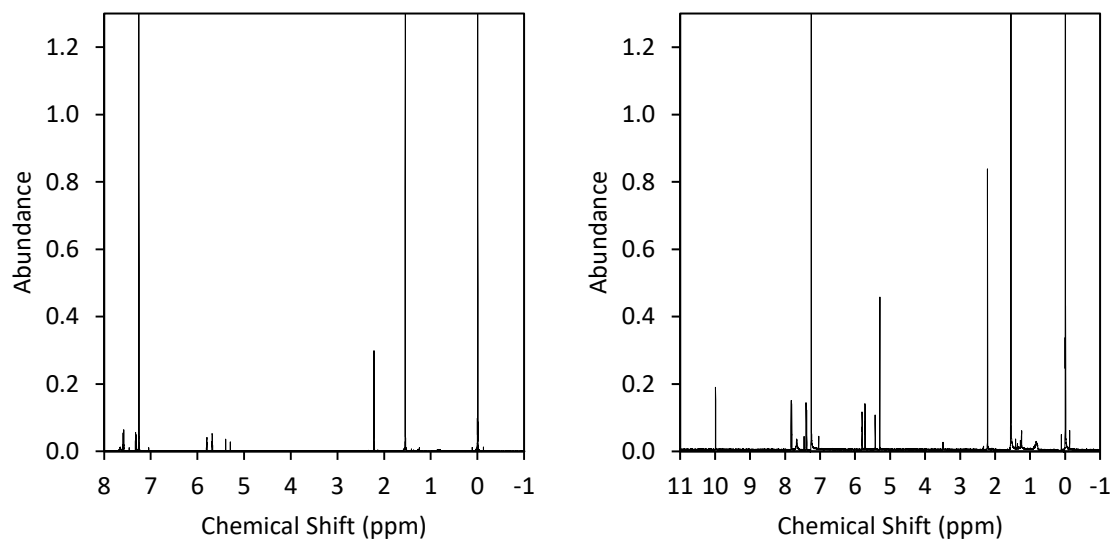
Figure 2-2. (A) ^{1}H-NMR spectrum of (1) in CDCl$_3$ and (B) ^{1}H-NMR spectrum of (2) in CDCl$_3$.

2.4.3 4,4-Difluoro-3,5-dimethyl-8-(4-formylphenyl)-4-bora-3a,4a-diaza-s-indacene (3)

In a 100 mL round-bottom flask, **2** (1.9 g, 6.83 mmol) was dissolved in dichloromethane (51 mL) and degassed for 10 min. The solution was treated with DDQ (1.7 g, 7.5 mmol) and stirred for 3 h at room temperature while being monitored with TLC. Red solid precipitated out of solution. Triethylamine (4.75 mL, 34 mmol) was added dropwise into the solution and stirred for 15 min dissolving the red precipitate. This was followed by the dropwise addition of boron trifluoride diethyl etherate (4.21 mL, 34 mmol) and a 3-h stir at room temperature. Vacuum filtration was then performed using celite. The crude product was then purified using column chromatography (silica, CH$_2$Cl$_2$) and a red solid was collected (652 mg, 30 %). The product was verified using UV-vis (Figure 2-3A) and ^{1}H-NMR analysis (Figure 2-3B).

Yield = 652 mg (30 %)

UV-vis (CH$_2$Cl$_2$) λ_{max}/nm: 332, 515

18

R_f (silica, CH_2Cl_2): 0.76

^{1}H-NMR (500 MHz, CDCl_3): δ, ppm: 10.12 (s, 1H, CHO); 8.00 (d, 2H, Ar-H); 7.66 (d, 2H, Ar-H); 6.64 (d, 2H, β -pyrrole); 6.29 (d, 2H, β -pyrrole); 2.66 (s, 6H, CH_3).
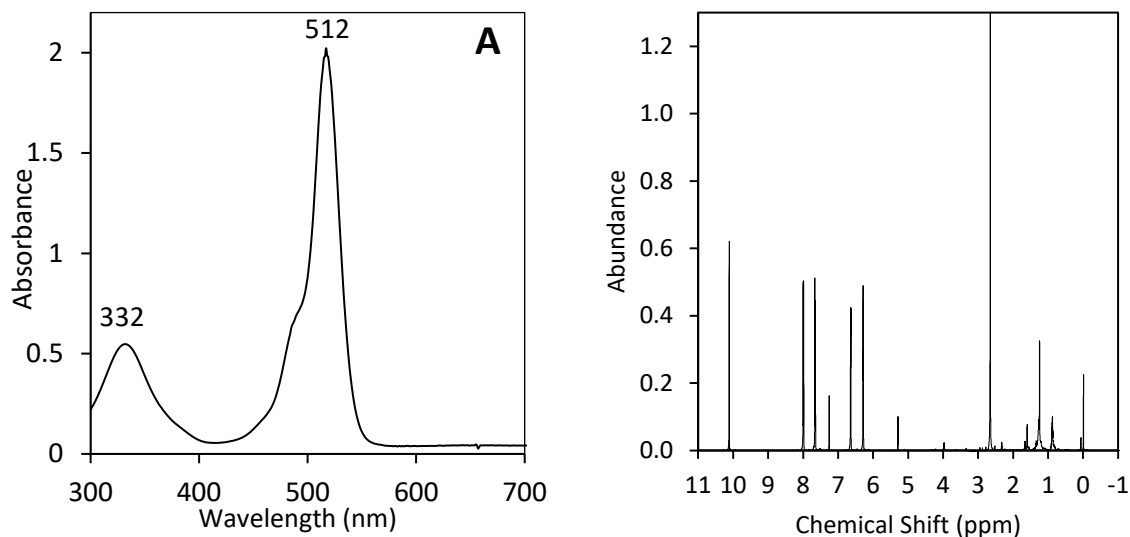
Figure 2-3. (A) UV-vis spectrum of 3 in CH_2Cl_2.; (B) ^{1}H-NMR spectrum of 3 in CDCl_3

2.5 **Synthesis of 5,10,15,20-tetrakis-(4,4-difluoro-3,5-dimethyl-4-bora-3a,4a-diaza-s-indacenephenyl)porphyrin, H_2(L-Por) (4)**
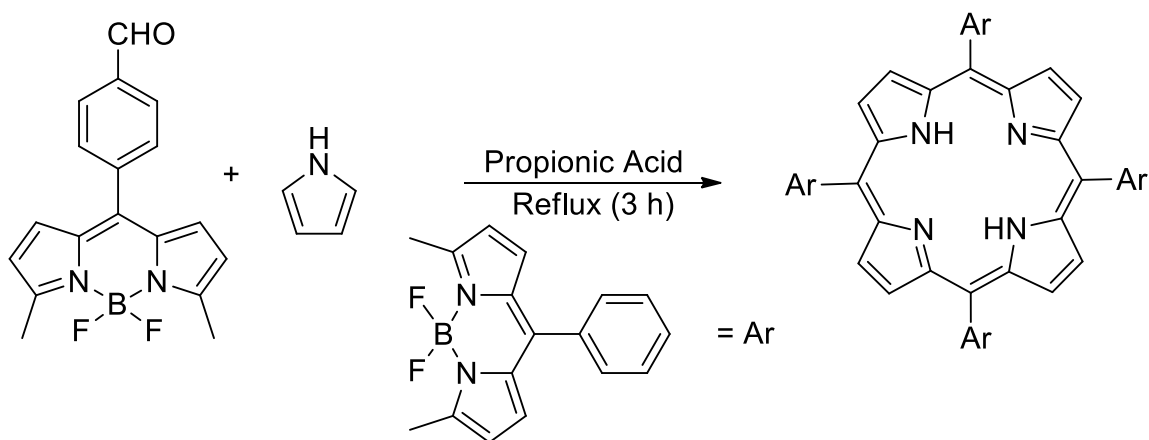
Scheme 2-2. Single-step synthesis of light-harvesting porphyrin.

Using the previously reported method by Adler et al., the light-harvesting porphyrin ligand was synthesized. The light-harvesting benzaldehyde **3** (250 mg, 0.77 mmol) and freshly distilled pyrrole (54 μL, 0.77 mmol) was added to 10 mL of propionic acid and refluxed. The solution was allowed to cool to room temperature then removed to an ice bath to promote recrystallization. The precipitate was collected via vacuum filtration using cold methanol to wash the product. The crude product was purified using column chromatography (silica, dichloromethane/hexanes) and a red product was collected and analyzed with UV-vis and ^{1}H-NMR. (Figure 2-4)

Yield = 33 mg (11.5 %)

UV-vis (CH_2Cl_2) λ_{max}/nm: 358, 420 (Soret) 514

^{1}H-NMR (500MHz, CDCl3): δ, ppm: 8.97 (s, 8H, β -pyrrole); 8.39 (d, 8H, Ar-H); 7.95 (d, 8H, Ar-H); 7.12 (d, 8H, β -pyrrole); 6.45 (d, 8H, β -pyrrole); 2.76 (s, 24H, CH3); -2.69 (s, 2H, inner-H)
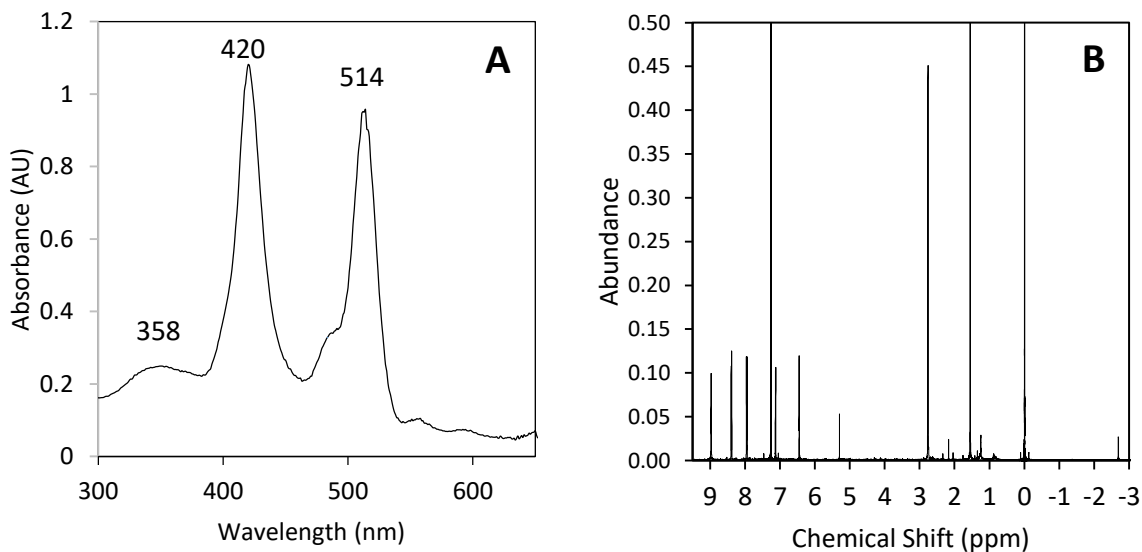
Figure 2-4. (A) UV-vis spectrum of (4) in CH_2Cl_2 and (B)^{1}H-NMR spectrum of (4) in CDCl$_3$

2.6 Synthesis of ruthenium(II) carbonyl light-harvesting porphyrin [Ru^{II}(L-Por)](CO)] (5)
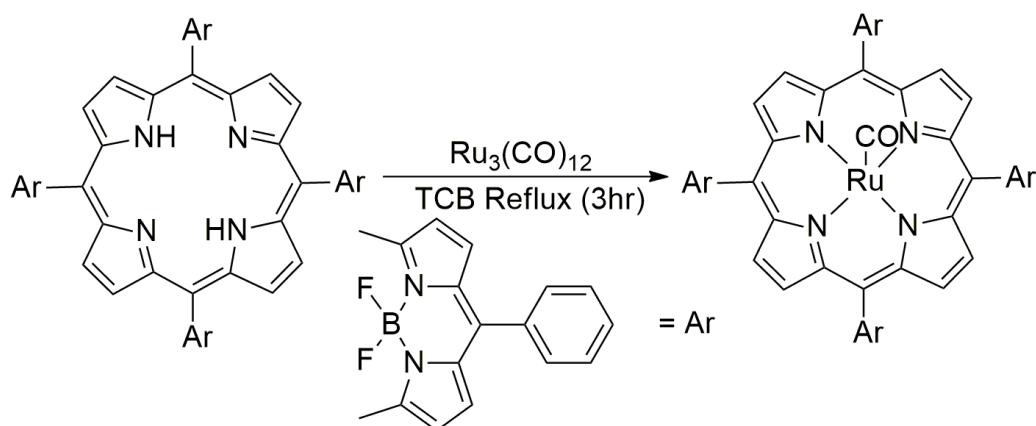
Scheme 2-3 Synthesis of ruthenium light-harvesting porphyrin [Ru^{II}(L-Por)(CO)]

The free ligand (30.5 mg) was dissolved in 25 mL of 1,2,4-trichlorobenzene and degassed for 10 min with argon in a 50 mL round bottom flask fitted with a reflux condenser. Triruthenium dodecacarbonyl salt (30.5 mg) were added to the solution while refluxing at 220°C and continued until TLC shows all free ligand has been consumed. The refluxing was then continued for an additional 20 min. The 1,2,4-trichlorobenzene was removed from the product via a neutral alumina column flushed with hexane (200-300 mL). A TLC plate under UV light was used to detect the presence of 1,2,4-trichlorobenzene. Dichloromethane was then used to elute the desired product. The product was characterized by UV-vis and ^{1}H-NMR.

Yield = 23 mg (69.4 %)

UV-vis (CH$_2$Cl$_2$) λ_{max}/nm: 339, 411 (Soret) 514

^{1}H-NMR (500MHz, CDCl$_3$): δ, ppm: 8.80 (s, 8H, β-pyrrole); 8.35 (d, 4H, Ar-H); 8.30 (d, 4H, Ar-H) 7.89 (d, 8H, Ar-H); 7.1 (d, 8H, β-pyrrole); 6.43 (d, 8H, β-pyrrole); 2.78 (s, 24H, CH$_3$)

2.7   Synthesis of iron(III) light-harvesting porphyrin Fe^{III}[(L-Por)](Cl) (6)

Figure 2-5. (A) ^{1}H-NMR spectrum of (5) in CDCl$_3$ and (B) UV-vis spectrum of (5) in CH$_2$Cl$_2$
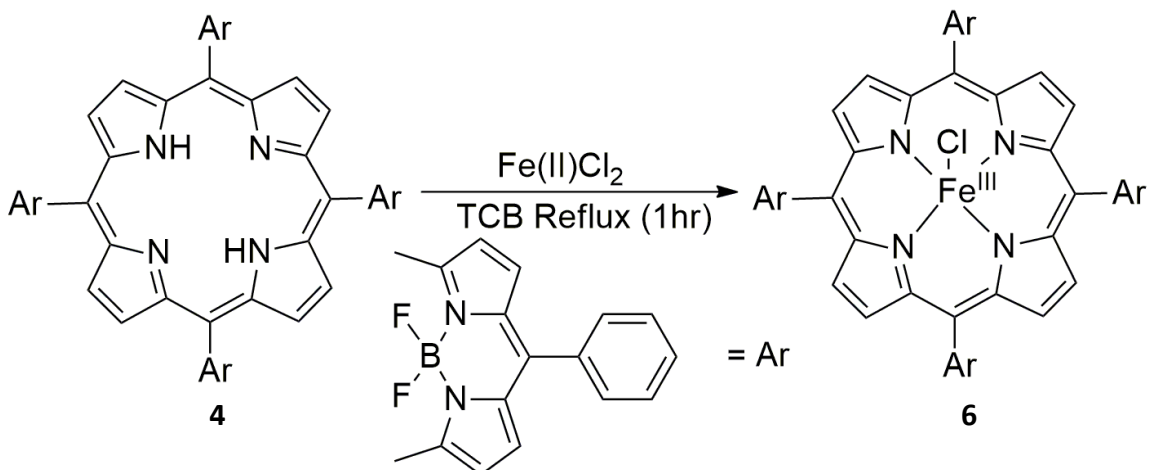
Scheme 2-4. Synthesis of iron light-harvesting porphyrin Fe^{III}(L-Por)CO (6)

The free ligand (40 mg) was dissolved in 20 mL of 1,2,4-trichlorobenzene and degassed for 10 min with Argon in a 100 mL round bottom flask with a condenser. Excess amounts of iron(II) chloride salt (120 mg) were added to the solution and refluxed for 80 min at 220°C (Scheme 1-1). The solution was monitored by UV-vis spectrometry based on changes in the Soret band. The 1,2,4-trichlorobenzene was removed from the product via

a neutral alumina column that was flushed with 200-300 mL of hexane. A TLC plate under UV light was used to check for the presence of 1,2,4-trichlorobenzene using hexane as the eluent. Dichloromethane was then used to elute the desired product. The product was stirred in 6 M hydrochloric acid for 30 minutes to insert the chlorine axial ligand. Extraction via separatory funnel was used to isolate the product and was monitored using litmus paper. The product was dried with sodium sulfate and the solvent was removed using rotary evaporation and characterized by UV-vis and ^{1}H-NMR (Figure 2-6).

R_f (silica, CH_2Cl_2): 0.6

UV-vis (CH_2Cl_2): λ_{max}/nm: 351, 514, (Soret), 420

^{1}H-NMR (500MHz, $CDCl_3$): δ, ppm: 82 ppm, (s, 8H, β-pyrrole);

Figure 2-6. (A) UV-vis spectrum of (**6**) in CH_2Cl_2 and (B) ^{1}H-NMR spectrum of (**6**) in $CDCl_3$

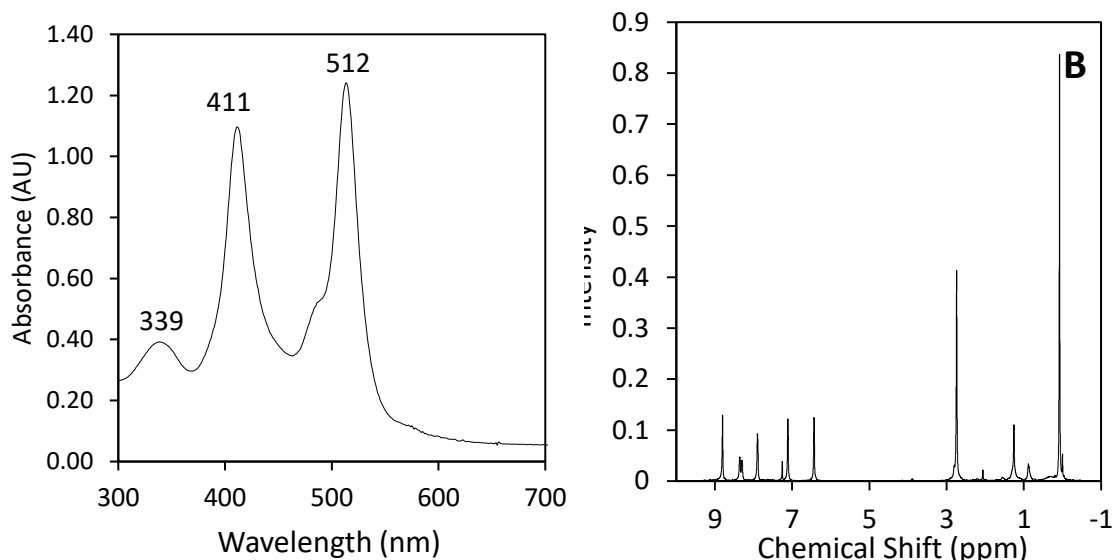## 2.8   Synthesis of Manganese(III) Light-Harvesting Porphyrin [Mn^{III}(L-Por)Cl] (7)
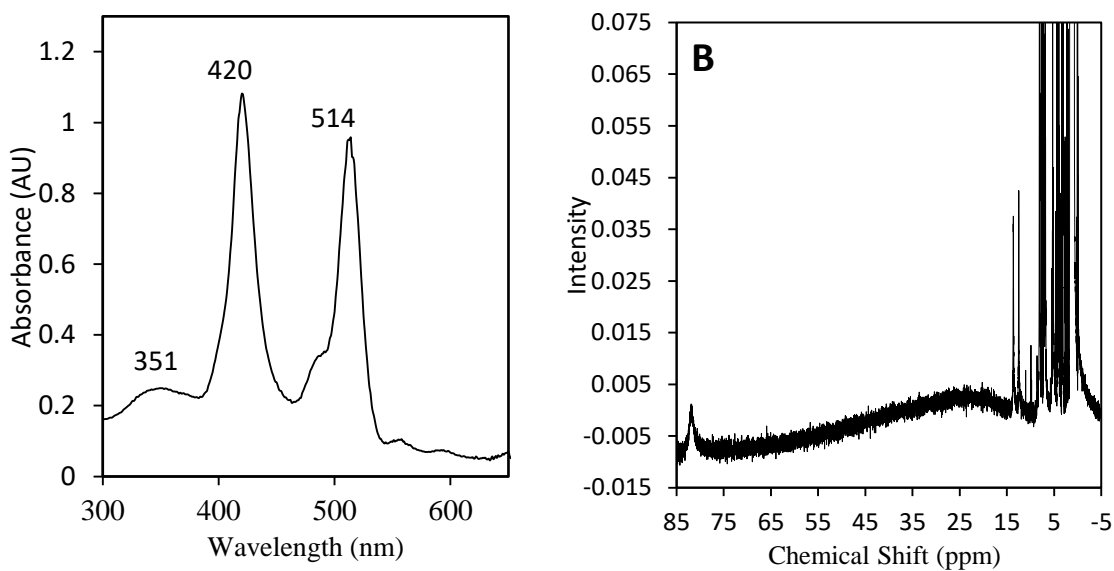
The free ligand (40 mg) was dissolved in 50mL of 1,2,4-trichlorobenzene and degassed for 10 minutes with Argon in a 100 mL round bottom flask with a condenser. Excess amounts of manganese(II) acetate tetrahydrate salt (340 mg) was added to the solution and refluxed for 30 min at 220°C (Scheme 1-2). The solution was monitored by UV-vis spectrometry based on changes in the Soret band. The 1,2,4-thrichlorobenzene was removed from the product via a neutral alumina column that was flushed with 200-300 mL of hexane. A TLC plate under UV light was used to check for the presence of 1,2,4-trichlorobenzene using hexane as the eluent. Dichloromethane was then used to elute unreacted free ligand. A dichloromethane/acetone mix was used to collect the desired product. The solvent was removed using rotary evaporation and characterized by UV-vis and ^{1}H-NMR (Figure 2-7)
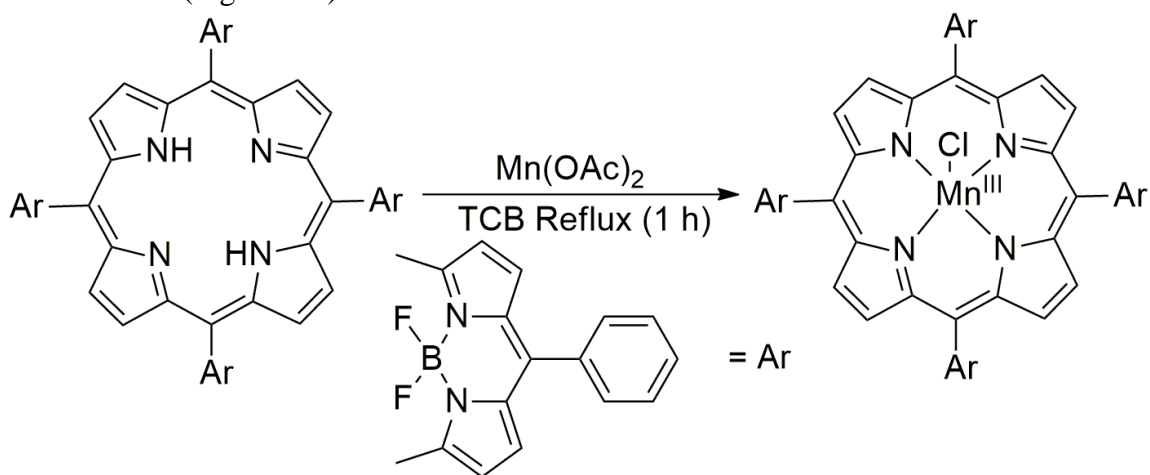
Scheme 2-5 Synthesis of manganese light-harvesting porphyrin [Mn^{III}(L-Por)Cl] (7)

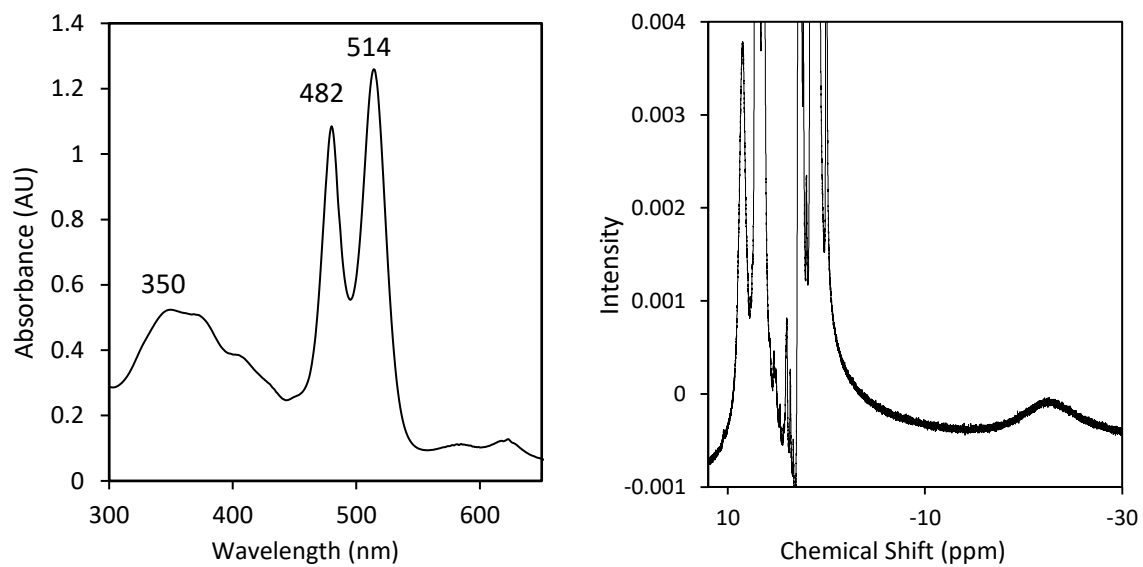R_f (silica, CH$_2$Cl$_2$/Acetone): 0.88

UV-vis (CH$_2$Cl$_2$): λ_{max}/nm: 350, 514, (Soret), 482

H-NMR (500MHz, CDCl$_3$): δ, ppm: -23 ppm, (s, 8H, β-pyrrole);

Figure 2-7. (A) UV-vis spectrum of **7** in CH_2Cl_2 and (B) ^1H-NMR spectrum of **7** in CDCl$_3$

CHAPTER 3

INVESTIGATION OF NOVEL LIGHT-HARVESTING PORPHYRIN FOR

ORGANIC SUBSTRATE OXIDATION

3.1   Introduction

Catalytic oxidation of organic compounds is a key process in industry for pharmaceuticals and fine chemical production.[67–69] In Nature, significant oxidation processes are often carried out through high-valent metal-oxo complexes as the premier oxidant. Cytochrome P450 (CYP450) stands as an excellent example, being found within most living organisms, it is able to catalyze the oxidation of a wide variety of substrates with high reactivity and selectivity.[70–72] The active site responsible for this oxidative capability is the iron protoporphyrin IX core. Over the past several decades, extensive effort has been invested into the design and experimentation of transition metalloporphyrin catalysts as P450 models for use in selective oxidation.[7–10] These biomimetic models tend to employ metals such as ruthenium, iron, and manganese as the porphyrin metal core.[73–75] The formed high-valent metal-oxo intermediates have demonstrated their ability to oxidize organic substrates at high efficiencies and selectivities, even for the functionalization of hydrocarbons.[71,76]

Previous studies conducted by our research lab established that ruthenium(II) porphyrin catalysts undergo an enhancement in catalytic efficiency upon irradiation of visible light for the oxidation of sulfides with iodobenzene diacetate as a mild oxygen source.[76] These CYP450 biomimetic models possess strong light absorbance due to the large π-system within the macrocycle and tend to capture light energy in a narrow range

within the region between 420 to 480 nm. This light energy aids in the formation of the metal-oxo intermediates acting as the oxygen atom transfer (OAT) species.[76] In order to expand the region in which more light energy may be captured, a modified porphyrin structure has been outfitted with boron-dipyrrin (BODIPY) dyes acting as light-harvesting antennae substituents located on the *meso*-positions of the porphyrin macrocycle.[77,78] The BODIPY antennae is expected to absorb wavelengths of light beyond that which the normal porphyrin core absorbs and transfer the energy to the core allowed by the spectral overlap of the antennae fluorescence and the porphyrin core absorbance spectra.[79] In this chapter, we have explored the photophysical properties and oxidative capabilities of three novel light-harvesting porphyrin complexes bearing a ruthenium, iron, or manganese atom as the metalloporphyrin center.

3.2   Photophysical properties

In order to ascertain if the introduction of the BODIPY substituent into the porphyrin structure successfully allows for absorption of a greater range of light forming a multichromophoric array, UV-vis spectroscopy was utilized to compare the absorption spectra of the light-harvesting porphyrin free ligand (**4**) and two reference compounds equivalent to the porphyrin macrocycle and BODIPY moiety. Figure 3-1 displays the normalized absorption spectra for **4** in CH_2Cl_2 overlaid with the absorption spectra of the BODIPY aldehyde (**3**) and the tetraphenyl porphyrin (H_2TPP), prepared as reported by Adler.[33] As shown, the absorption spectrum of **4** possesses three distinct absorption bands at 358, 420, and 514 nm, as well as the porphyrin Q-bands in the 500 to 600 nm region.
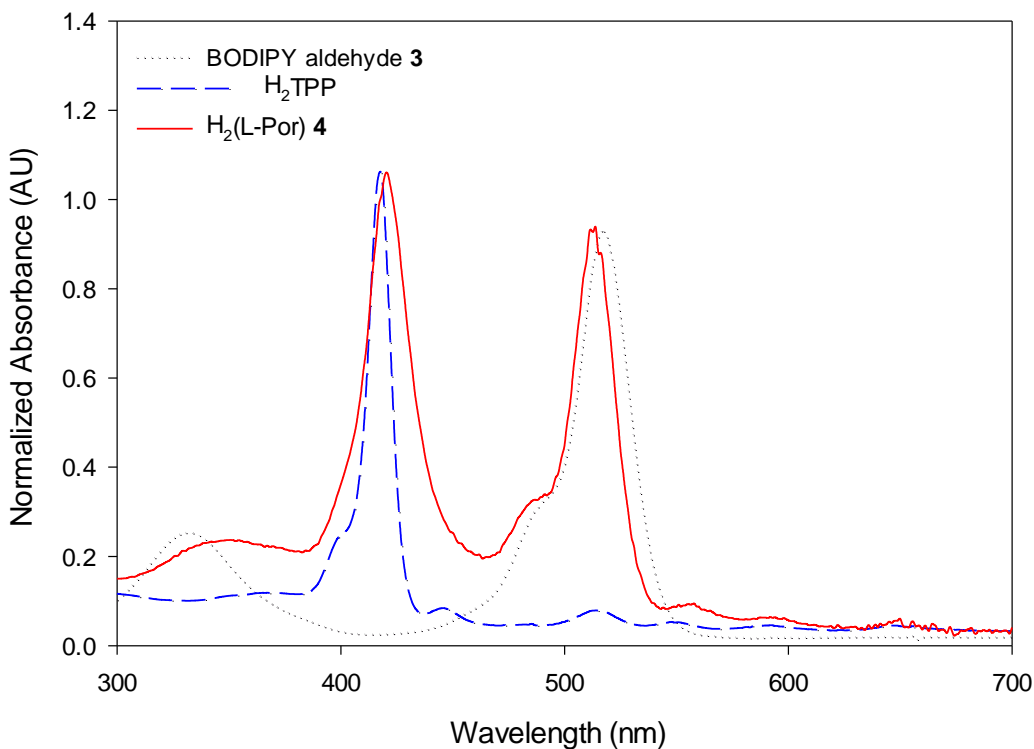
Figure 3-1. Normalized UV-vis spectra of BODIPY aldehyde (dotted line), light-harvesting porphyrin (solid line), and H$_2$TPP (dashed line). The spectra of 3 and 4 were normalized at 512 nm; the spectra of 4 and H$_2$TPP were normalized at 418 nm**.**

In comparison to H$_2$TPP acting as an unsubstituted free ligand analog, **4** is absorbing a larger region of light in the visible spectrum. There is significant spectral overlap between H$_2$(L-Por) and the two reference compounds where the absorbance spectrum of **4** is approximately the summation of the two reference spectra. This implies the incorporation of the BODIPY moiety into the porphyrin structure does not result in ground state interactions between the two chromophores.[80] The UV-vis spectrum of **5** shows similar peak absorbance values to that of **4** with only a blue shift of the porphyrin Soret band from 420 to 411 nm consistent with previously reported observations,[81] as well as a redshift of the peak at 358 nm to 339 nm (Fig 3-2).
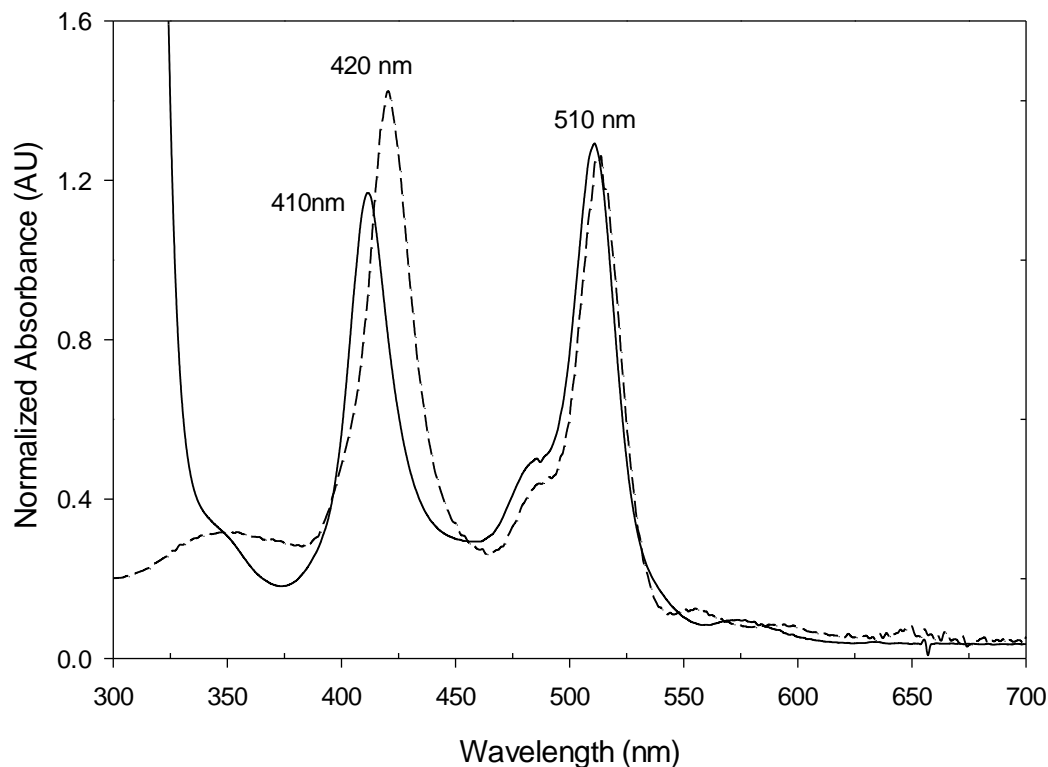
Figure 3-2. UV-vis spectra of light-harvesting porphyrin **4** (dashed line) and [Ru^{II}(L-Por)(CO)] **5** (solid line).

Figure 3-3A displays the fluorescent emission spectra of the **3** and **4** both excited at 510 nm in CH$_2$Cl$_2$. As shown, **3** displays a strong emission at 544 nm while **4** only demonstrates fluorescence only at 654 and 720 nm. Likewise, the ruthenium(II) carbonyl porphyrin complex (**5**) displays a similar fluorescence spectrum to that of the free ligand with an addition emission at 421 nm (Fig 3-3B). The lack of fluorescence for both **4** and **5** within a similar range as **3** suggests an internal energy transfer process within the light-harvesting porphyrin structure.[82] The overlap of the fluorescent emission spectrum of the BODIPY moiety with the Q-band absorbance region between 500 and 600 nm may allow for non-radiative energy transfer from the peripheral BODIPY chromophores to the porphyrin core via Förster resonance energy transfer (FRET).[83]
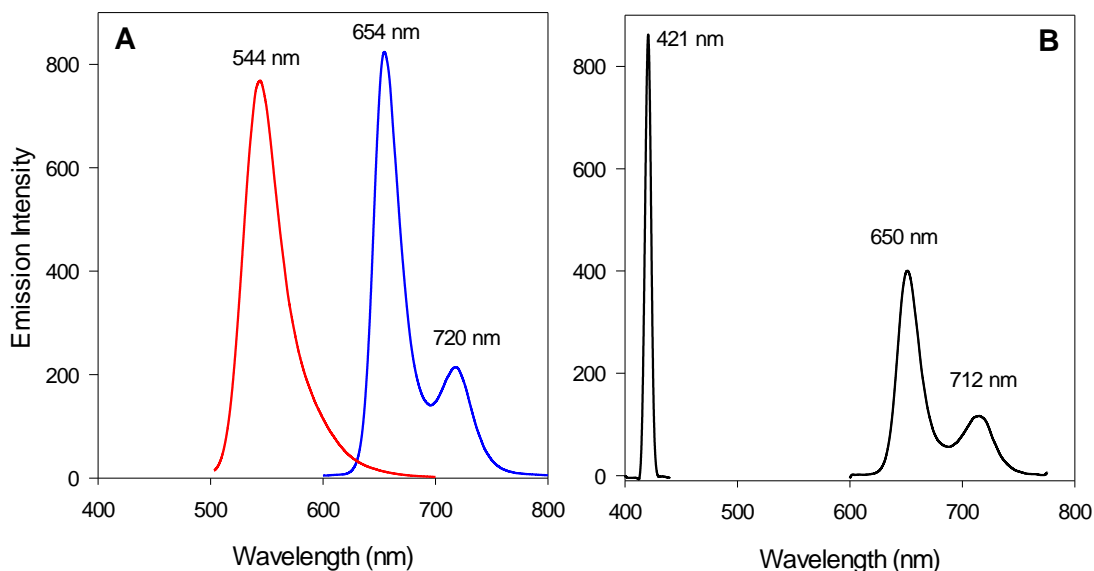
Figure 3-3. (A) Fluorescence spectra of **3** (red) and **4** (blue) in CH$_2$Cl$_2$ at equal absorbance at 515 nm, both excited at 510 nm. (B) Fluorescence spectrum of **5** in CH$_2$Cl$_2$ excited at 419 nm.

3.3   Visible light-induced formation and kinetic studies of high-valent manganese(IV)-oxo light-harvesting porphyrin [Mn^{IV}(L-Por)O]

3.3.1   Chemical generation of [Mn^{IV}(L-Por)O]

Generation of the high-valent manganese(IV)-oxo (**8**) intermediate was performed through the chemical oxidation of manganese(III) light-harvesting porphyrin (**7**) upon the addition of the sacrificial oxidant iodobenzene diacetate [PhI(OAc)$_2$] in excess (Scheme 3-1). Figure 3-4A displays time-resolved spectra of the formation of the Mn^{IV}(L-Por)O from the oxidation of Mn^{III}(L-Por) with 10 equivalents of PhI(OAc)$_2$ over 1 s in CH$_3$CN. The growth of the 428 nm peak is indicative of the formation of the Mn^{IV}-oxo species being consistent with the Soret band of previous Mn^{IV}-oxo porphyrin species.[75] Further

indication is given by the decay of the previously characterized Mn^{III}(L-Por) Soret band at 480 nm.
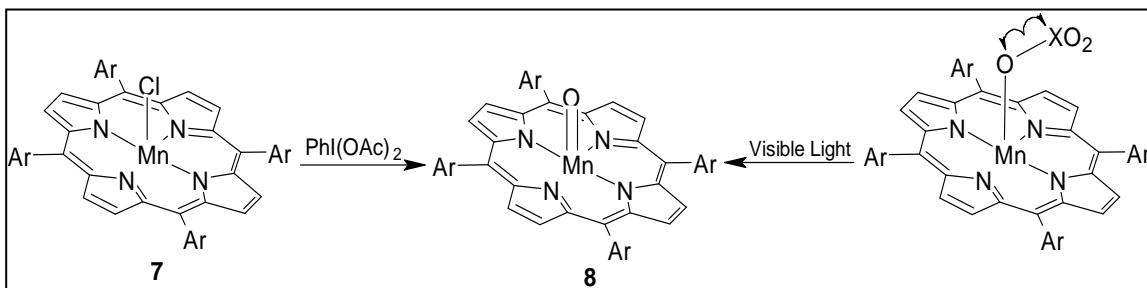
Scheme 3-1. Chemical formation (left) and photochemical formation (right) of manganese(IV)-oxo porphyrin.
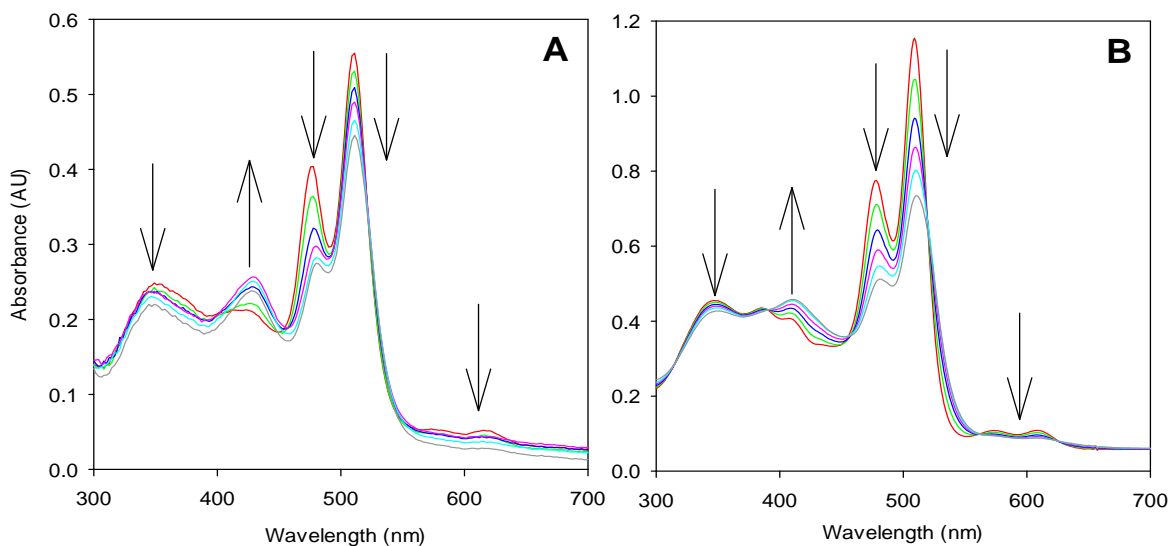
Figure 3-4. (A) Time-resolved spectra of [Mn^{IV}(L-Por)O] following the chemical oxidation of [Mn^{III}(L-Por)Cl] in CH$_3$CN with PhI(OAc)$_2$ (10 equiv.) over 1s. (B) Time-resolved spectra of [Mn^{IV}(L-Por)O]following photochemical oxidation of [Mn^{III}(L-Por)(ClO$_3$)] in CH$_3$CN with 100 equiv. of AgClO$_3$ over 35s.

3.3.2 Photochemical generation of [Mn^{IV}(L-Por)O]

Three distinct manganese-salt complexes were generated from **7** upon the addition of excess inorganic salts: silver chlorate, silver bromate, or silver nitrite. The edition of one of these silver salts in solution with **7** leads to the formation of highly photo-labile manganese chlorate, bromate, or nitrite salts. Photolysis of these manganese salt complexes is induced upon irradiation with visible light. The irradiation leads to homolytic cleavage of the O-X (X = Cl, Br, or N) to yield Mn^{IV}(L-Por)O (**8**). Figure 3-4B displays the time-resolved spectra of formation of Mn^{IV}-oxo intermediates upon photolysis using visible light on manganese chlorate complex. The Mn^{IV}-oxo intermediate formed by visible light photolysis on all three salt complexes exhibits the similar spectral signature, matching those chemically generated by oxidation of **7** with PhI(OAc)$_2$. Therefore, it can be concluded that both methods of oxidation produce the same oxide product.

3.3.3 Kinetic studies of [Mn^{IV}(L-Por)O]

Time-resolved spectra and kinetic studies of the oxidation of thioanisole using the chemically-generated [Mn^{IV}(L-Por)O] intermediate were undertaken. Figure 3-5A displayed a time-resolved spectrum of the high-valent Mn^{IV}-oxo intermediate **8** reacting with thioanisole (0.1M) in CH$_3$CN and reforming the [Mn^{III}(L-Por)]. The spectra show the decay of the Mn^{IV} Soret band at 428 nm and growth of the Mn^{III} Soret band at 480 nm. Several rate constants were obtained for the reaction of **8** with varying concentrations of thioanisole in CH$_3$CN and 10 equivalence of PhI(OAc)$_2$. A kinetic plot was created from the rate constants observed from the reaction of **8** with various concentrations of the substrate thioanisole where the observed rate constants increased as a function of substrate

concentration (Fig. 3-5B). The plot displays a linear relationship where the slope gave the second-order rate constant as k_{ox} $(M^{-1}s^{-1})$ = 0.4158. This is a much slower rate than predicted. Rates of previous manganese(IV)-oxo porphyrins demonstrate a reaction rate of at least a magnitude higher for the oxidation of thioanisole.[84]
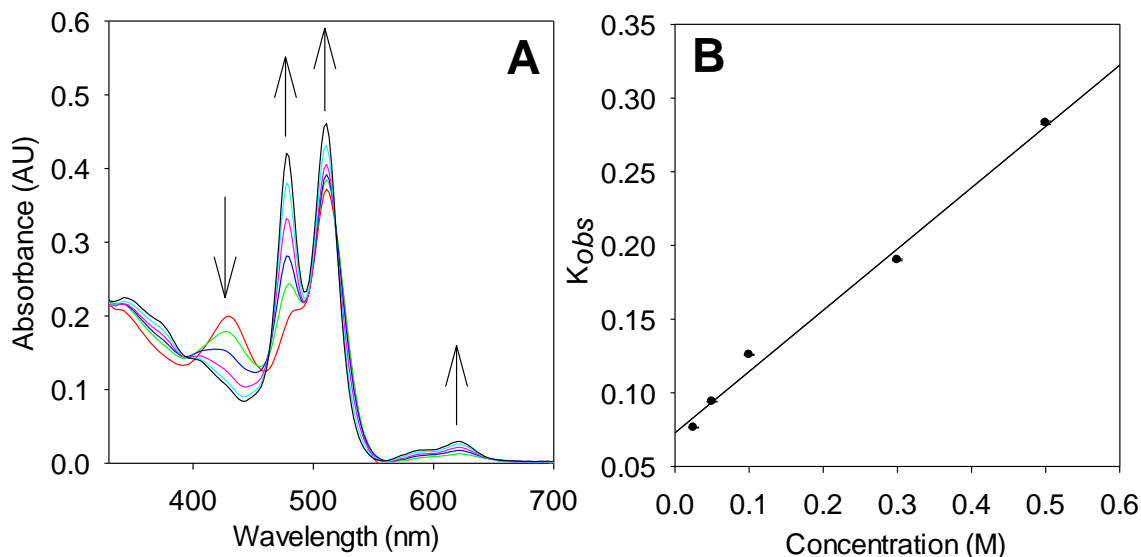
Figure 3-5. (A) Time-resolved spectra of [Mn^{IV}(L-Por)O] reacting in CH$_3$CN with thioanisole (0.1M) and PhI(OAc)$_2$ (10 equiv.) over 40s. (B) Kinetic plots of the observed rate constants of [Mn^{IV}(L-Por)O] versus the concentration of thioanisole in CH$_3$CN with PhI(OAc)$_2$ (10 equiv.).

3.4   Catalytic oxidations using novel light-harvesting metalloporphyrins

3.4.1   Catalytic oxidations using [Ru^{II}(L-Por)(CO)] (5)

Previous studies have demonstrated the ability of ruthenium(II) carbonyl porphyrins to undergo photo-induced decarbonylation to generate a more reactive form of the Ru^{II} catalyst. Therefore, all oxidation trials were carried out under visible light irradiation.[76] Various *p*-substituted thioanisoles were utilized as substrates to investigate the efficiency of the ruthenium light-harvesting porphyrin for sulfoxidation in optimal

conditions. All sulfoxidations were performed in CH$_3$OH in the presence of a small amount of water (4.5 µL). PhI(OAc)$_2$ acted as the mild oxygen source with 1.5 equivalence of substrate ensuring full conversion of substrates to products. Only 0.2 mol% of **5** was used for these reactions (Table 3-1). Excellent oxidation efficiency is observed in nearly all cases with complete conversions of substrate to product being reached in less than 2 h in many cases. This is a noticeable advancement in efficiency compared to similar to ruthenium(II) porphyrin complexes without the BODIPY moiety utilized in previous studies.
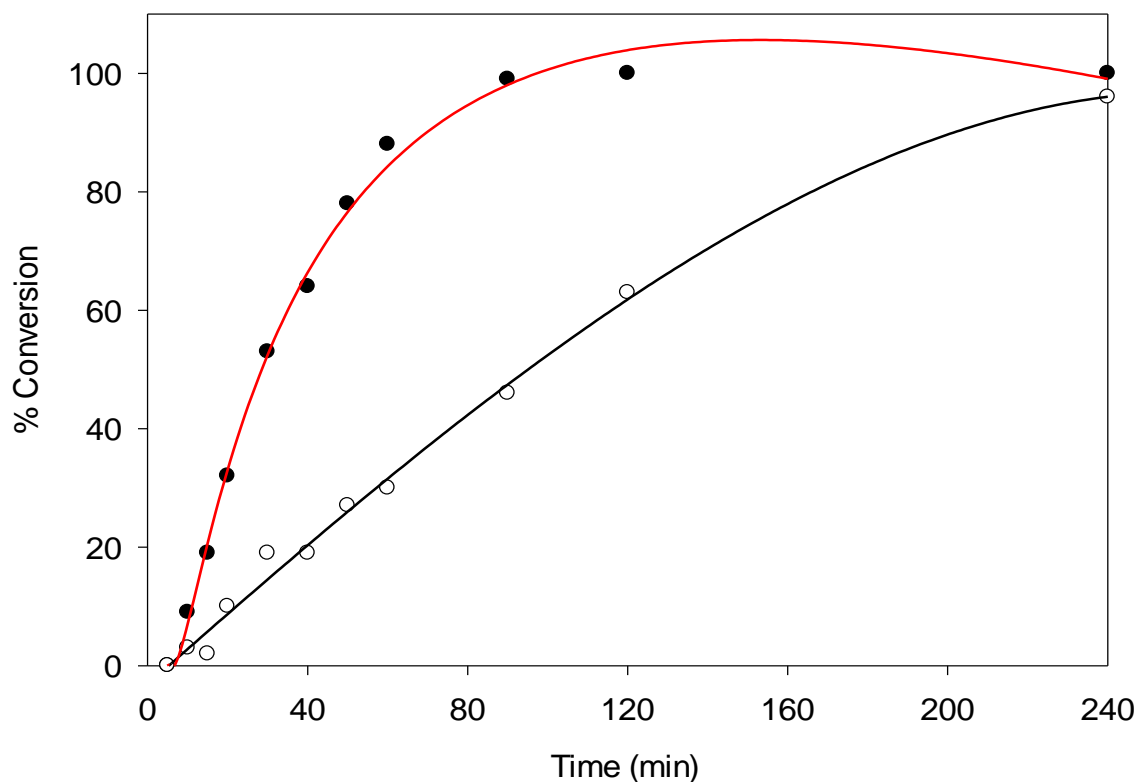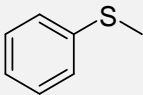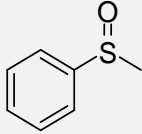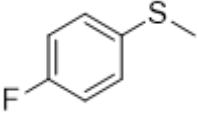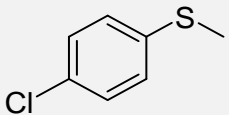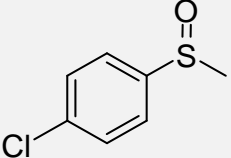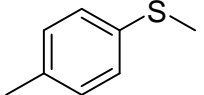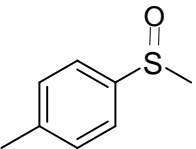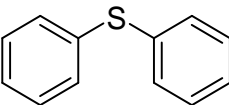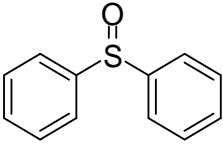
Figure 3-6. Time courses of oxidation of thioanisole (0.5 mmol) with PhI(OAc)$_2$ (0.75 mmol) in CH$_3$OH (2 mL) at room temperature catalyzed by ruthenium(II) porphyrin 5 (1 mmol) in the presence of H$_2$O (4.5 mL) with visible light (red line with black circle) and without visible light (black line with white circle).

Thioanisole oxidation with **5** under visible light is shown to reach near full conversion within 1.5 h whereas [Ru^{II}(TMP)(CO)] is considerably slower requiring 6 h for complete conversion where TMP is tetrametsitylporphyrin. Also observed throughout the trials is good to excellent selectivity for sulfoxide over sulfone. As displayed in Fig. 6, the conversion efficiency of **5** considerably increases with exposure to visible light. This noticeable light effect is observed for all substrates.
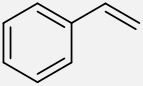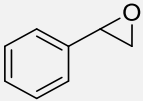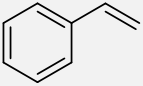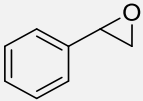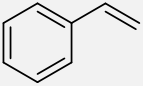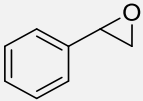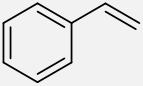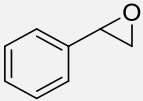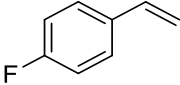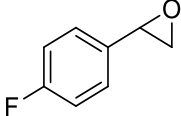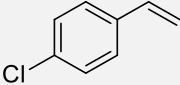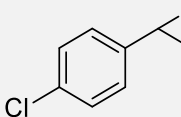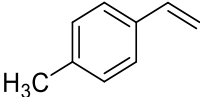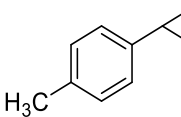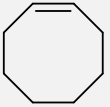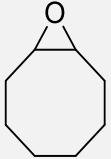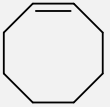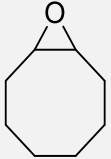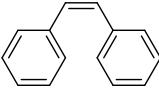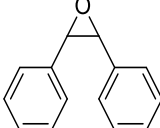
Also investigated was the catalytic potential of **5** for the epoxidation of various alkenes. Due to the efficiency with which ruthenium porphyrins have been able to catalyz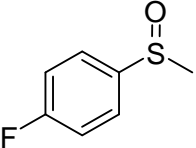e the oxidation of hydrocarbons and olefins using substituted pyridine *N*-oxides, 2,6-dichloropyridine *N*-oxide (Cl$_2$pyNO) was chosen as the oxygen source for these epoxidation trials (Table 3-2).[85,86] The Cl$_2$pyNO was administered in a 1 to 1.1 ratio of substrate to oxygen source (0.5 mmol to 0.55 mmol) along with 0.5 µmol of catalyst.

Similar to the sulfoxidation trials, an increase in epoxidation efficiency under visible light irradiation can be seen (Table 3-2, entries 1 and 2). The oxidation of styrene with **5** yields an 88% conversion after 6 h. In the same conditions, less than 5% of styrene is transformed to its corresponding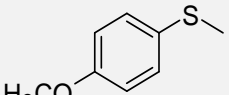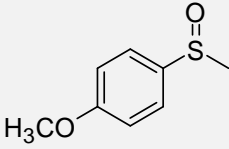 oxide without light. As well, all olefin oxidation trials yielded excellent selectivity. Both *cis*-stilbene and *cis*-cyclooctene demonstrated complete stereoretention for the oxide product. However, changing the solvent from CH$_2$Cl$_2$ to toluene or dichloroethane (entries 3-4 in Table 3-2) led to catalyst degradation and a decrease in conversion rates.

Table 3-1 Catalytic sulfoxidation for sulfide substrates by RuII(L-Por)(CO).[a]

Entry	Substrate	Time (min)	Conv.[b] (%)	Product	Selectivity[c]	TON
1		90	100		92:08	460
2[d]		240	97		93:07	451
3		60	97		96:04	466
4		60	96		85:15	408
5		75	100		87:13	435
6		90	100		88:12	440
7		120	50		76:24	190

[a] All reactions were conducted with visible light irradiation (λmax = 420nm) in a Rayonet reactor or otherwise noted. All reactions were performed in CH_3OH (2 mL) at ca. 23°C with 1.5 equiv. of PhI(OAc)$_2$ (0.75 mmol), substrate (0.5 mmol), 0.2 mol% catalyst in the presence of H_2O (4.5μL); only sulfoxide and small amounts of sulfone were detected by GC-MS analysis of the crude reaction mixture [b] Based on the conversion from substrate to products [c] Ratio of products (sulfoxide : sulfone). [d] Without visible light irradiation.

Table 3-2 Catalytic epoxidation for alkene substrates by RuII(L-Por)(CO).[a]

Entry	Substrate	Time (h)	Conv.[b] (%)	Product	Selectivity[c]	TON
1		6	88.2		95.3	841
2[d]		6	< 2		> 99%	n.d.
3[e]		6	64.3		97.9	630
4[f]		3	55.5		95.1	480
5		6	41.0		94.3	387
6		6	74.7		97.0	725
7		6	22.4		81.8	183
8		6	34.8		98.4	171
9[d]		6	< 1		n.d.	n.d.
10		6	38.2		98.4	376

[a] All reactions were conducted under visible light irradiation (λ_{max} = 420nm) in a Rayonet reactor or otherwise noted. All reactions were performed in CH_2Cl_2 (2 mL) at ca. 23°C with 1.1 equiv. of 2,6-Cl$_2$PyNO (0.55 mmol), substrate (0.5 mmol), 0.1 mol% catalyst (0.5 μmol); only epoxide and small amounts of phenyl acetaldehyde were detected by GC-MS analysis of the crude reaction mixture. [b] Based on the conversion from substrate to products. [c] Yield of epoxide. [d] Without visible light irradiation [e] Reaction was conducted in toluene (2 mL). [f] Reaction was conducted in dichloroethane (2 mL).
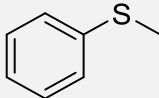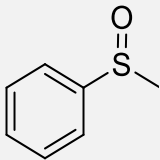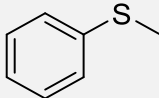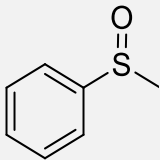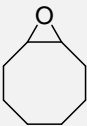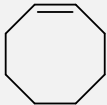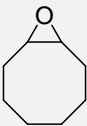
3.4.2 Catalytic oxidations using [Fe^{III}(L-Por)Cl] (6)

Preliminary oxidation trials were performed using this new iron(III) light-harvesting porphyrin chloride in a similar manner as with **5**. High-valent iron porphyrins are found commonly throughout Nature such as in biological catalytic cycles of specific proteins such as CYP450 which possesses a heme cofactor as the active site. Iron porphyrin complexes tend to be more widely used than their manganese or ruthenium counterparts toward substrate oxidations. Unsubstituted thioanisole was chosen as the substrate of focus for oxidation trials using two different catalyst loads. As seen in Table 3-3 entries 3 and 4, a catalyst load of 0.15 mol% was prepared. This is of the same magnitude as that of **5** and **7** used for the oxidation of thioanisole. The result was 85% conversion in 5 min with and without light as well as excellent selectivity. A second catalyst load of 0.015 mol% was prepared and resulted in full conversion reached within 1 h with excellent selectivity. Oxidation of thioanisole using **6** was found to be far more efficient than with either **5** or **7** with much greater TON. A strong increase in catalytic efficiency with exposure to visible light suggests an increase in efficiency of the catalyst due to enhanced light absorbance due to the multichromophoric array.

In contrast, *cis*-cyclooctene epoxidation did not proceed well with only 6.3% conversion after 1 h with light. The reaction was conducted in a similar manner as **5** and **6** in 2 mL of chloroform with 0.5 mol% catalyst loading with *cis*-cyclooctene (0.2 mmol) and 1.5 equivalence of PhI(OAc)$_2$ (0.3 mmol) as the oxygen source in the presence of water (4.5 µL). While selectivity was excellent with only the epoxide being detected by GC-MS analysis, it yielded poor catalytic efficiency. As can be seen, the ideal conditions for this iron porphyrin catalysis trial have not yet been discovered.

It is possible that the light source used for these reactions may have been too strong, leading to catalyst bleaching or transformation into a less active species. As well, substituting the *ortho* positions of the phenyl ring attached to the dipyrrin moiety with a bulky substituent will prevent the formation of a potential stable dimeric species that may be interfering with the oxidation. Further experimentation with differing solvents, substrates, substituents and light sources may improve the catalytic efficiency of the iron light-harvesting catalyst.

Table 3-3 Catalytic sulfoxidation for sulfide substrates by FeIII(L-Por)Cl.[a]

Entry	Substrate	Time (min)	Conv.[b] (%)	Product	Selectivity[c]	TON
1		60	99.5		96:04	6368
2[d]		60	42.9		96:04	2746
3[e]		5	84.7		97:03	548
4[de]		5	86.9		97:03	561
5[f]		60	6.3		100	13
6[df]		60	2.8		100	6

[a] All reactions were conducted with visible light irradiation (λmax = 420nm) in a Rayonet reactor or otherwise noted. All reactions were performed in $CHCl_3$ (2 mL) at ca. 23°C with 1.5 equiv. of $PhI(OAc)_2$ (0.75 mmol), substrate (0.5 mmol), 0.015 mol% catalyst (0.075 µmol) in the presence of H_2O (4.5µL); only sulfoxide and small amounts of sulfone were detected by GC-MS analysis of the crude reaction mixture. [b] Based on the conversion from substrate to products. [c] Ratio of products (substrate : oxide). [d] Without visible light irradiation. [e] 0.15 mol% catalyst (0.75 µmol) loading. [f] Reaction was performed in CH_2Cl_2 (2 mL) at ca. 23°C with 1.5 equiv. of $PhI(OAc)_2$ (0.3 mmol), substrate (0.2 mmol), 0.5

mol% catalyst (1.0 µmol) in the presence of H_2O (4.5µL); only epoxide was detected by GC-MS analysis of the crude reaction mixture.

3.4.3 Catalytic oxidations using [Mn^{III}(L-Por)Cl] (7)
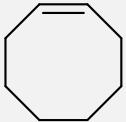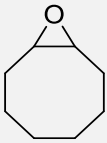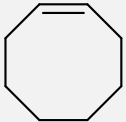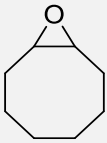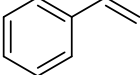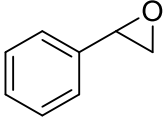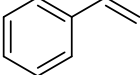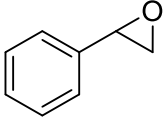
Preliminary oxidation trials were conducted using **7** in a manner similar to **5** and **6** (Table 3-4) Unsubstituted thioanisole (0.5 mmol) was selected as the substrate for sulfoxidation by **7** (0.2 mol%) using 1.5 equivalence of PhI(OAc)$_2$ (0.75 mmol) in CHCl$_3$ (2 mL) in the presence of a small amount of water (4.5 µL). The results were poor conversion near 30% in 1 h with good selectivity. No appreciable accelerating effect was found upon exposure to light.
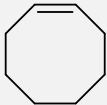
Table 3-4 Catalytic sulfoxidation for sulfide substrates by Mn^{III}(L-Por)Cl.[a]

Entry	Substrate	Time (min)	Conv.[b] (%)	Product	Selectivity[c]	TON
1		60	24.3		85:15	103
2[d]		60	27.2		84:16	114
3[e]		60	32.9		74:26	162
4[de]		60	37.6		80:20	201

[a] All reactions were conducted with visible light irradiation (λmax = 420nm) in a Rayonet reactor or otherwise noted. All reactions were performed in CHCl$_3$ (2 mL) at ca. 23°C with 1.5 equiv. of PhI(OAc)$_2$ (0.75 mmol), substrate (0.5 mmol), 0.2 mol% catalyst (1.0 µmol) in the presence of H_2O (4.5µL); only sulfoxide and small amounts of sulfone were detected by GC-MS analysis of the crude reaction mixture. [b] Based on the conversion from substrate to products. [c] Ratio of products (sulfoxide : sulfone). [d] Without visible light irradiation. [e] 0.15 mol% catalyst (0.75 µmol) loading.

Table 3-5 Catalytic epoxidation for alkene substrates by [Mn^{III}(L-Por)Cl].[a]

Entry	Substrate	Time (h)	Conv.[b] (%)	Product	Selectivity [c]	TON
1		1	12.5		100	25
2[d]		1	7.7		100	15
3		6	14.9		100	30
4[d]		6	10.3		100	21

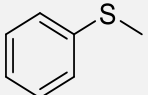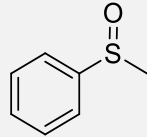[a] All reactions were conducted with visible light irradiation (λmax = 420nm) in a Rayonet reactor or otherwise noted. All reactions were performed in CH$_2$Cl$_2$ (2 mL) at ca. 23°C with 1.5 equiv. of PhI(OAc)$_2$ (0.3 mmol), substrate (0.2 mmol), 0.5 mol% catalyst (1.0 µmol) in the presence of H$_2$O (4.5µL) [b] Based on the conversion from substrate to products. [c] Yield of epoxide. [d] Without visible light irradiation.

Epoxidation using **7** gave similar results to the sulfoxidation trials. Epoxidation trials were performed with *cis*-cyclooctene (0.2 mmol) as substrate with 1.5 equivalence of PhI(OAc)$_2$ (0.3 mmol) as the oxygen source in CH$_2$Cl$_2$. 0.5 mol% of catalyst was introduced in the presence of water (4.5 µL). The results were less than 15% conversion with or without light after 1 hour. A similar trial was conducted with styrene with less than 15% conversion after 6 h. The small difference of epoxide yields between trials with and without light may indicate a mild light accelerating effect. Likely there exists similar reasoning for the lack of reactivity for both the manganese porphyrin-catalyzed reactions and the iron porphyrin-catalyzed epoxidation. The potential formation of a stable dimeric species has not yet been disproved and may be investigated in the future. As well, it is likely that the oxidation trials were not being performed in optimal conditions for the catalysts and so further experimentation with varying light-sources, substrates, and solvents may potentially lead to improved catalytic efficiency.

Chapter 4

CONCLUSION

In summary, a popular organic fluorophore, boron dipyrrin (BODIPY) was successfully synthesized as an efficient light-harvesting unit that can be linked to metalloporphyrin complexes. The fluorophore was incorporated as a substituent on the porphyrin scaffolding to act as an antenna to capture a broad range of visible light. In this work, ruthenium, iron, and manganese complexes supported by the light-harvesting BODIPY-porphyrin ligand have been successfully synthesized and characterized for the first time.

Florescence spectrometry was utilized to identify the overlap of the fluorescence spectrum of the light-harvesting BODIPY substituent with the absorption spectrum of the porphyrin chromophore at the Q band region, which fulfills the requirements for excited energy transfer (EET) of the light energy absorbed by the antennae system to the reaction center through the Förster mechanism. This is expected to increase the efficiency at which these compounds catalyze oxidative transformations. As well, time resolved spectra for the formation of the manganese(IV)-oxo intermediate has been collected for both chemical and photochemical oxidation mechanisms in which it is shown that both methods result in the formation of the same oxidant species.

Preliminary oxidation trials were conducted with each of the novel metalloporphyrin catalysts. Ruthenium light-harvesting porphyrin displayed a remarkable catalytic activity for the oxidation of both sulfides and alkenes, demonstrating a definite light accelerating effect in catalytic activity upon visible light irradiation. In contrast, the

manganese and iron complexes did not show light enhanced effects on epoxidation and sulfoxidation reactions.

The future of this research is to investigate this novel method of enhancing the light-harvesting capability of metalloporphyrin and further improve the efficiency at which these biomimetic photocatalysts operate. Future investigations into light-harvesting metalloporphyrin will seek to identify the best possible reaction conditions for catalytic oxidation trials for these complexes such as performing screening studies as well as identifying possible solvent effects and substrate scope. Modifications of the substituent structure to alter the electronic environment of the catalyst, such as the addition of electron-withdrawing substituents onto the *ortho* positions of the phenyl rings connected to the dipyrrin, may further enhance the catalytic capabilities of these light-harvesting compounds.

REFERENCES

(1)   Mueller, G. C.; Miller, J. A. The Metabolism of 4-Dimethylaminoazobenzene by Rat Liver Homogenates. *J. Biol. Chem.* **1948**, *176* (Copyright (C) 2019 American Chemical Society (ACS). All Rights Reserved.), 535–544.

(2)   Axelrod, J. THE ENZYMATIC DEMETHYLATION OF EPHEDRINE. *J Pharmacol Exp Ther* **1955**, *114* (4), 430.

(3)   Brodie, B. B.; Axelrod, J.; Cooper, J. R.; Gaudette, L.; La Du, B. N.; Mitoma, C.; Udenfriend, S. Detoxication of Drugs and Other Foreign Compounds by Liver Microsomes. *Science* **1955**, *121* (3147), 603–604.

(4)   Garfinkel, D. Studies on Pig Liver Microsomes. I. Enzymic and Pigment Composition of Different Microsomal Fractions. *Archives of Biochemistry and Biophysics* **1958**, *77* (2), 493–509.

(5)   Klingenberg, M. Pigments of Rat Liver Microsomes. *Archives of Biochemistry and Biophysics* **1958**, *75* (2), 376–386.

(6)   Omura, T.; Sato, R. A New Cytochrome in Liver Microsomes. *Journal of Biological Chemistry* **1962**, *237* (4), PC1375–PC1376.

(7)   Omura, T.; Sato, R. The Carbon Monoxide-Binding Pigment of Liver Microsomes. *Journal of Biological Chemistry* **1964**, *239* (7), 2370–2378.

(8)   Denisov, I. G.; Makris, T. M.; Sligar, S. G.; Schlichting, I. Structure and Chemistry of Cytochrome P450. *Chem. Rev.* **2005**, *105* (6), 2253–2278.

(9)   Guengerich, F. P. Cytochrome P450 and Chemical Toxicology. *Chem. Res. Toxicol.* **2008**, *21* (1), 70–83.

(10) Nebert, D. W.; Russell, D. W. Clinical Importance of the Cytochromes P450. *The Lancet* **2002**, *360* (9340), 1155–1162.

(11) Scott, E. E. ω- versus (ω-1)-Hydroxylation: Cytochrome P450 4B1 Sterics Make the Call. *Journal of Biological Chemistry* **2017**, *292* (13), 5622–5623.

(12) Meunier, B.; de Visser, S. P.; Shaik, S. Mechanism of Oxidation Reactions Catalyzed by Cytochrome P450 Enzymes. *Chem. Rev.* **2004**, *104* (9), 3947–3980.

(13) Ji, H.-B.; Zhou, X.-T. Biomimetic Homogeneous Oxidation Catalyzed by Metalloporphyrins with Green Oxidants. In *Biomimetics Learning from Nature*; Mukherjee, A., Ed.; InTech, 2010.

(14) Burnham, B. F.; Plane, R. A. Studies on the Biosynthesis of the Corrin Ring of Vitamin B12. *Biochemical Journal* **1966**, *98* (1), 13C-15C.

(15) Borah, K. D.; Bhuyan, J. Magnesium Porphyrins with Relevance to Chlorophylls. *Dalton Trans.* **2017**, *46* (20), 6497–6509.

(16) Gray, H. B.; Winkler, J. R. Living with Oxygen. *Acc. Chem. Res.* **2018**, *51* (8), 1850–1857.

(17) Ji, H.-B.; Zhou, X.-T. Biomimetic Homogeneous Oxidation Catalyzed by Metalloporphyrins with Green Oxidants. *Biomimetics Learning from Nature* **2010**.

(18) Erdogan, H. One Small Step for Cytochrome P450 in Its Catalytic Cycle, One Giant Leap for Enzymology. *J. Porphyrins Phthalocyanines* **2019**, *23* (04n05), 358–366.

(19) Mak, P. J.; Denisov, I. G. Spectroscopic Studies of the Cytochrome P450 Reaction Mechanisms. *Biochimica et Biophysica Acta (BBA) - Proteins and Proteomics* **2018**, *1866* (1), 178–204.

(20) Denisov, I. G.; Mak, P. J.; Makris, T. M.; Sligar, S. G.; Kincaid, J. R. Resonance Raman Characterization of the Peroxo and Hydroperoxo Intermediates in Cytochrome P450 [†]. *J. Phys. Chem. A* **2008**, *112* (50), 13172–13179.

(21) Loida, P. J.; Sligar, S. G. Molecular Recognition in Cytochrome P-450: Mechanism for the Control of Uncoupling Reactions. *Biochemistry* **1993**, *32* (43), 11530–11538.

(22) Groves, J. T.; McClusky, G. A.; White, R. E.; Coon, M. J. Aliphatic Hydroxylation by Highly Purified Liver Microsomal Cytochrome P-450. Evidence for a Carbon Radical Intermediate. *Biochemical and Biophysical Research Communications* **1978**, *81* (1), 154–160.

(23) Fertinger, C.; Hessenauer-Ilicheva, N.; Franke, A.; van Eldik, R. Direct Comparison of the Reactivity of Model Complexes for Compounds 0, I, and II in Oxygenation, Hydrogen-Abstraction, and Hydride-Transfer Processes. *Chemistry - A European Journal* **2009**, *15* (48), 13435–13440.

(24) Ogliaro, F. The Experimentally Elusive Oxidant of Cytochrome P450: A Theoretical "Trapping" Defining More Closely the "Real" Species. **2001**, No. 11, 4.

(25) Ogliaro, F.; de Visser, S. P.; Cohen, S.; Sharma, P. K.; Shaik, S. Searching for the Second Oxidant in the Catalytic Cycle of Cytochrome P450: A Theoretical Investigation of the Iron(III)-Hydroperoxo Species and Its Epoxidation Pathways. *J. Am. Chem. Soc.* **2002**, *124* (11), 2806–2817.

(26) Groves, J. T.; Nemo, T. E.; Myers, R. S. Hydroxylation and Epoxidation Catalyzed by Iron-Porphine Complexes. Oxygen Transfer from Iodosylbenzene. *J. Am. Chem. Soc.* **1979**, *101* (4), 1032–1033.

(27) Barona-Castaño, J. C.; Carmona-Vargas, C. C.; Brocksom, T. J.; De Oliveira, K. T. Porphyrins as Catalysts in Scalable Organic Reactions. *Molecules* **2016**, *21* (3), 310.

(28) Chang, C. K.; Kuo, M.-S. Reaction of Iron(III) Porphyrins and Iodosoxylene. The Active Oxene Complex of Cytochrome P-450. *J. Am. Chem. Soc.* **1979**, *101* (12), 3413–3415.

(29) Rothemund, P. A New Porphyrin Synthesis. The Synthesis of Porphin [1]. *J. Am. Chem. Soc.* **1936**, *58* (4), 625–627.

(30) Pereira, M. M.; Dias, L. D.; Calvete, M. J. F. Metalloporphyrins: Bioinspired Oxidation Catalysts. *ACS Catal.* **2018**, *8* (11), 10784–10808.

(31) Dolphin, D.; Traylor, T. G.; Xie, L. Y. Polyhaloporphyrins: Unusual Ligands for Metals and Metal-Catalyzed Oxidations. *Acc. Chem. Res.* **1997**, *30* (6), 251–259.

(32) Adler, A. D.; Longo, F. R.; Shergalis, William. Mechanistic Investigations of Porphyrin Syntheses. I. Preliminary Studies on *Ms* -Tetraphenylporphin. *J. Am. Chem. Soc.* **1964**, *86* (15), 3145–3149.

(33) Adler, A. A Simplified Synthesis for Meso-Tetraphenylporphyrin. *J. Org. Chem.* **1967**, *32* (2), 476–477.

(34) Lindsey, J. S.; Hsu, H. C.; Schreiman, I. C. Synthesis of Tetraphenylporphyrins under Very Mild Conditions. *Tetrahedron Letters* **1986**, *27* (41), 4969–4970.

(35)   Lindsey, J. S.; Schreiman, I. C.; Hsu, H. C.; Kearney, P. C.; Marguerettaz, A. M. Rothemund and Adler-Longo Reactions Revisited: Synthesis of Tetraphenylporphyrins under Equilibrium Conditions. *J. Org. Chem.* **1987**, *52* (5), 827–836.

(36)   Zhang, R.; Vanover, E.; Chen, T.-H.; Thompson, H. Visible Light-Driven Aerobic Oxidation Catalyzed by a Diiron(IV) µ-Oxo Biscorrole Complex. *Applied Catalysis A: General* **2013**, *464–465*, 95–100.

(37)   Newcomb, M.; Zhang, R.; Chandrasena, R. E. P.; Halgrimson, J. A.; Horner, J. H.; Makris, T. M.; Sligar, S. G. Cytochrome P450 Compound I. *J. Am. Chem. Soc.* **2006**, *128* (14), 4580–4581.

(38)   Kwong, K. W.; Patel, D.; Malone, J.; Lee, N. F.; Kash, B.; Zhang, R. An Investigation of Ligand Effects on the Visible Light-Induced Formation of Porphyrin–Iron(IV)-Oxo Intermediates. *New J. Chem.* **2017**, *41* (23), 14334–14341.

(39)   Traylor, T. G.; Tsuchiya, S. Perhalogenated Tetraphenylhemins: Stable Catalysts of High Turnover Catalytic Hydroxylations. *Inorg. Chem.* **1987**, *26* (8), 1338–1339.

(40)   Gross, Z.; Gray, H. B. Oxidations Catalyzed by Metallocorroles. *Advanced Synthesis & Catalysis* **2004**, *346* (23), 165–170.

(41)   Costas, M. Selective C–H Oxidation Catalyzed by Metalloporphyrins. *Coordination Chemistry Reviews* **2011**, *255* (23), 2912–2932.

(42) Groves, J. T.; Kruper, W. J.; Haushalter, R. C. Hydrocarbon Oxidations with Oxometalloporphinates. Isolation and Reactions of a (Porphinato)Manganese(V) Complex. *J. Am. Chem. Soc.* **1980**, *102* (20), 6375–6377.

(43) Zhang, J.-L.; Che, C.-M. Dichlororuthenium(IV) Complex Ofmeso-Tetrakis(2,6-Dichlorophenyl)Porphyrin: Active and Robust Catalyst for Highly Selective Oxidation of Arenes, Unsaturated Steroids, and Electron-Deficient Alkenes by Using 2,6-DichloropyridineN-Oxide. *Chem. Eur. J.* **2005**, *11* (13), 3899–3914.

(44) Zhang, R.; Newcomb, M. Laser Flash Photolysis Formation and Direct Kinetic Studies of Manganese(V)-Oxo Porphyrin Intermediates. *J. Am. Chem. Soc.* **2003**, *125* (41), 12418–12419.

(45) Malone, J.; Klaine, S.; Alcantar, C.; Bratcher, F.; Zhang, R. Synthesis of a Light-Harvesting Ruthenium Porphyrin Complex Substituted with BODIPY Units. Implications for Visible Light-Promoted Catalytic Oxidations. *New J. Chem.* **2021**.

(46) Zhang, R.; Vanover, E.; Luo, W.; Newcomb, M. Photochemical Generation and Kinetic Studies of a Putative Porphyrin-Ruthenium(∨)-Oxo Species. *Dalton Trans.* **2014**, *43* (23), 8749–8756.

(47) Vanover, E.; Huang, Y.; Xu, L.; Newcomb, M.; Zhang, R. Photocatalytic Aerobic Oxidation by a Bis-Porphyrin−Ruthenium(IV) μ-Oxo Dimer: Observation of a Putative Porphyrin−Ruthenium(V)−Oxo Intermediate. *Org. Lett.* **2010**, *12* (10), 2246–2249.

(48) Hermans, I.; Spier, E. S.; Neuenschwander, U.; Turrà, N.; Baiker, A. Selective Oxidation Catalysis: Opportunities and Challenges. *Top Catal* **2009**, *52* (9), 1162–1174.

(49) Wittcoff, H.; Reuben, B. G.; Plotkin, J. S. *Industrial Organic Chemicals*, 2nd ed.; Wiley-Interscience: Hoboken, N.J, 2004.

(50) Teles, J. H.; Hermans, I.; Franz, G.; Sheldon, R. A. Oxidation. In *Ullmann's Encyclopedia of Industrial Chemistry*; American Cancer Society, 2015; pp 1–103.

(51) Shilov, A. E.; Shul'pin, G. B. Activation of C−H Bonds by Metal Complexes. *Chem. Rev.* **1997**, *97* (8), 2879–2932.

(52) Parshall, G. W.; Ittel, S. D. *Homogeneous Catalysis*; Wiley, 1992.

(53) Carreno, M. Carmen. Applications of Sulfoxides to Asymmetric Synthesis of Biologically Active Compounds. *Chem. Rev.* **1995**, *95* (6), 1717–1760.

(54) Okabe, S.; Shimosako, K.; Amagase, K. PHARMACOLOGICAL REGULATION OF GASTRIC ACID SECRETION IN THE APICAL MEMBRANE OF PARIETAL CELLS; A NEW TARGET FOR ANTISECRETORY DRUGS. 18.

(55) Cai, Y.; Wang, R.; Pei, F.; Liang, B.-B. Antibacterial Activity of Allicin Alone and in Combination with B-Lactams against Staphylococcus Spp. and Pseudomonas Aeruginosa. 4.

(56) Zifko, U. A.; Rupp, M.; Schwarz, S.; Zipko, H. T.; Maida, E. M. Modafinil in Treatment of Fatigue in Multiple Sclerosis. *Journal of Neurology* **2002**, *249* (8), 983–987.

(57) Surendra, K.; Krishnaveni, N. S.; Kumar, V. P.; Sridhar, R.; Rao, K. R. Selective and Efficient Oxidation of Sulfides to Sulfoxides with N-Bromosuccinimide in the Presence of β-Cyclodextrin in Water. *Tetrahedron Letters* **2005**, *46* (27), 4581–4583.

(58) Trost, B. M.; Ley, S. V.; Fleming, I. *Oxidation*; Comprehensive Organic Synthesis II - Online; Elsevier Science, 1991.

(59) Nehlsen, J. P.; Benziger, J. B.; Kevrekidis, I. G. A Process for the Removal of Thiols from a Hydrocarbon Stream by a Heterogeneous Reaction with Lead Oxide. *Energy Fuels* **2004**, *18* (3), 721–726.

(60) Zhu, W.; Li, H.; Jiang, X.; Yan, Y.; Lu, J.; Xia, J. Oxidative Desulfurization of Fuels Catalyzed by Peroxotungsten and Peroxomolybdenum Complexes in Ionic Liquids. *Energy Fuels* **2007**, *21* (5), 2514–2516.

(61) Khan, M. R.; Sayed, E. 8 - Sulfur Removal from Heavy and Light Petroleum Hydrocarbon by Selective Oxidation. In *Advances in Clean Hydrocarbon Fuel Processing*; Khan, M. R., Ed.; Woodhead Publishing, 2011; pp 243–261.

(62) Armor, J. N. A History of Industrial Catalysis. *Catalysis Today* **2011**, *163* (1), 3–9.

(63) Toulhoat, H. Heterogeneous Catalysis: Use of Density Functional Theory. **2016**.

(64) Caron, S.; Dugger, R. W.; Ruggeri, S. G.; Ragan, J. A.; Ripin, D. H. B. Large-Scale Oxidations in the Pharmaceutical Industry [†]. *Chem. Rev.* **2006**, *106* (7), 2943–2989.

(65) Kaczorowska, K.; Kolarska, Z.; Mitka, K.; Kowalski, P. Oxidation of Sulfides to Sulfoxides. Part 2: Oxidation by Hydrogen Peroxide. *Tetrahedron* **2005**, *61* (35), 8315–8327.

(66) Miao, Q.; Shin, J.-Y.; Patrick, B. O.; Dolphin, D. Self-Assembly of Oligomeric Linear Dipyrromethene Metal Complexes. *Chem. Commun.* **2009**, No. 18, 2541.

(67) Huang, X.; Groves, J. T. Oxygen Activation and Radical Transformations in Heme Proteins and Metalloporphyrins. *Chem. Rev.* **2018**, *118* (5), 2491–2553.

(68) Bäckvall, J.-E. *Modern Oxidation Methods*; John Wiley & Sons, 2011.

(69) Punniyamurthy, T.; Velusamy, S.; Iqbal, J. Recent Advances in Transition Metal Catalyzed Oxidation of Organic Substrates with Molecular Oxygen. *Chem. Rev.* **2005**, *105* (6), 2329–2364.

(70) Groves, J. T. Models and Mechanisms of Cytochrome P450 Action. 43.

(71) Denisov, I. G.; Makris, T. M.; Sligar, S. G.; Schlichting, I. Structure and Chemistry of Cytochrome P450. *Chem. Rev.* **2005**, *105* (6), 2253–2278.

(72) Ortiz de Montellano, P. R.; De Voss, J. J. Oxidizing Species in the Mechanism of Cytochrome P450. *Nat. Prod. Rep.* **2002**, *19* (4), 477–493.

(73) Hoshino, Mikio.; Kashiwagi, Yasuhiro. Photoinduced Decarbonylation of Ruthenium(II) Carbonyl Octaethylporphyrin in Acetonitrile: Studies on the Origin of the Excitation Wavelength Dependence. *J. Phys. Chem.* **1990**, *94* (2), 673–678.

(74) Bartoli, J. F.; Brigaud, O.; Battioni, P.; Mansuy, D. Hydroxylation of Linear Alkanes Catalysed by Iron Porphyrins: Particular Efficacy and Regioselectivity of Perhalogenated Porphyrins. *J. Chem. Soc., Chem. Commun.* **1991**, No. 6, 440.

(75) Kwong, K. W.; Chen, T.-H.; Luo, W.; Jeddi, H.; Zhang, R. A Biomimetic Oxidation Catalyzed by Manganese(III) Porphyrins and Iodobenzene Diacetate: Synthetic and Mechanistic Investigations. *Inorganica Chimica Acta* **2015**, *430*, 176–183.

(76) Chen, T.-H.; Yuan, Z.; Carver, A.; Zhang, R. Visible Light-Promoted Selective Oxidation of Sulfides to Sulfoxides Catalyzed by Ruthenium Porphyrins with Iodobenzene Diacetate. *Applied Catalysis A: General* **2014**, *478*, 275–282.

(77)   Loudet, A.; Burgess, K. BODIPY Dyes and Their Derivatives: Syntheses and Spectroscopic Properties. *Chem. Rev.* **2007**, *107* (11), 4891–4932.

(78)   Prieto-Montero, R.; Prieto-Castañeda, A.; Sola-Llano, R.; Agarrabeitia, A. R.; García-Fresnadillo, D.; López-Arbeloa, I.; Villanueva, A.; Ortiz, M. J.; Moya, S.; Martínez-Martínez, V. Exploring BODIPY Derivatives as Singlet Oxygen Photosensitizers for PDT. *Photochem Photobiol* **2020**, *96* (3), 458–477.

(79)   Whited, M. T.; Djurovich, P. I.; Roberts, S. T.; Durrell, A. C.; Schlenker, C. W.; Bradforth, S. E.; Thompson, M. E. Singlet and Triplet Excitation Management in a Bichromophoric Near-Infrared-Phosphorescent BODIPY-Benzoporphyrin Platinum Complex. 9.

(80)   Erwin, P.; Conron, S. M.; Golden, J. H.; Allen, K.; Thompson, M. E. Implications of Multichromophoric Arrays in Organic Photovoltaics. *Chem. Mater.* **2015**, *27* (15), 5386–5392.

(81)   Che, C.-M.; Zhang, J.-L.; Zhang, R.; Huang, J.-S.; Lai, T.-S.; Tsui, W.-M.; Zhou, X.-G.; Zhou, Z.-Y.; Zhu, N.; Chang, C. K. Hydrocarbon Oxidation by β-Halogenated Dioxoruthenium(VI) Porphyrin Complexes: Effect of Reduction Potential (RuVI/V) and C□H Bond-Dissociation Energy on Rate Constants. *Chem. Eur. J.* **2005**, *11* (23), 7040–7053.

(82)   Leonardi, M. J.; Topka, M. R.; Dinolfo, P. H. Efficient Förster Resonance Energy Transfer in 1,2,3-Triazole Linked BODIPY-Zn(II) Meso-Tetraphenylporphyrin Donor–Acceptor Arrays. *Inorg. Chem.* **2012**, *51* (24), 13114–13122.

(83)   N. J. Turro. Chapter 9. In *Modern Molecular Photochemistry*; University Science Books: Sausalito, 1991.

(84) Klaine, S.; Bratcher, F.; Winchester, C. M.; Zhang, R. Formation and Kinetic Studies of Manganese(IV)-Oxo Porphyrins: Oxygen Atom Transfer Mechanism of Sulfide Oxidations. *Journal of Inorganic Biochemistry* **2020**, *204*, 110986.

(85) Hirobe, M.; Ohtake, H.; Higuchi, T. The Highly Efficient Oxidation of Olefins, Alcohols, Sulfides and Alkanes with Heteroaromatic N-Oxides Catalyzed by Ruthenium Porphyrins. *HETEROCYCLES* **1995**, *40* (2), 867.

(86) Wang, C.; Shalyaev, K. V.; Bonchio, M.; Carofiglio, T.; Groves, J. T. Fast Catalytic Hydroxylation of Hydrocarbons with Ruthenium Porphyrins. *Inorg. Chem.* **2006**, *45* (12), 4769–4782.